

AD-A068 004

OKLAHOMA UNIV NORMAN SCHOOL OF AEROSPACE MECHANICAL --ETC F/G 20/4
SUPERSONIC FLOW PAST CONICAL BODIES WITH NEARLY CIRCULAR CROSS---ETC(U)
OCT 78 M C JISCHKE
OU-AMNE-78-10

UNCLASSIFIED

AFOSR-TR-79-0475

NL

OF
AD
A068004



ADA068004

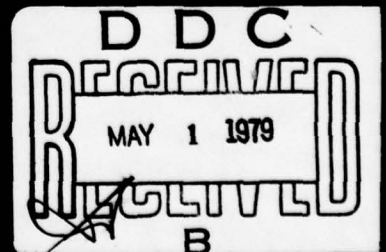
DDC FILE COPY

am
he

① LEVEL III

DISTRIBUTION STATEMENT A

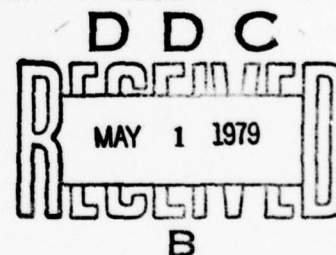
Approved for public release;
Distribution Unlimited



University of Oklahoma
School of Aerospace, Mechanical and Nuclear Engineering
Research Report No. OU-AMNE 78-10

SUPERSONIC FLOW PAST CONICAL BODIES
WITH NEARLY CIRCULAR CROSS-SECTIONS

by
Martin C. Jischke



Prepared for
USAF Office of Scientific Research under
Grant AFOSR 77-3468
OU ORA 158-005
October 1978

DISTRIBUTION STATEMENT A
Approved for public release;
Distribution Unlimited

AIR FORCE OFFICE OF SCIENTIFIC RESEARCH (AFOSR)
NOTICE OF TRANSMISSION TO DDC
This technical report has been reviewed and is
approved for public release IAW AFR 190-12 (7b).
Distribution is unlimited.
A. D. BLOSE
Technical Information Officer

PREFACE

This investigation was sponsored by the United States Air Force, Office of Scientific Research, under Grant No. AFOSR - 77-3468. This work was conducted by Professor Martin C. Jischke; School of Aerospace, Mechanical and Nuclear Engineering, University of Oklahoma; Norman, Oklahoma 73019. Dr. Martin Zimmer, AFOSR, and Dr. Donald Daniel, Eglin AFB, served as Project Monitors.

ACCESSION for		
NTIS	White Section	<input checked="checked" type="checkbox"/>
DDC	Buff Section	<input type="checkbox"/>
UNANNOUNCED		<input type="checkbox"/>
JUSTIFICATION _____		
BY _____		
DISTRIBUTION/AVAILABILITY CODES		
Dist.	Avail.	and/or SPECIAL
A		

ABSTRACT

Inviscid, supersonic conical flows past bodies whose cross-section deviates slightly from that of a right circular cone are studied by means of a perturbation technique. Writing the equation for the body as $\theta_b(\phi) = \theta_{o_b} + \sum \theta_{n_b} \cos n\phi + \sum \theta_{m_b} \sin m\phi$, where $\theta_{n_b}, \theta_{m_b} \ll \theta_{o_b}$, we have obtained analytical results with the assumption of a weak polar cross-flow (eg. $\vec{V} \cdot \hat{e}_\theta / a \ll 1$). The effects of small angles of attack and yaw are included. Using the hypersonic small disturbances theory approximations, we have developed explicit results for the flow field velocity components, pressure, entropy, and shock shape for cases $n, m = 1, 2, 3, 4$. Comparisons of theory with experiment for $n = 1, 2$ are favorable. The results obtained also agree with linearized theory when $M_1\theta \rightarrow 0$ and Newtonian theory when $M_1\theta \rightarrow \infty$. The streamsurfaces of the velocity field are calculated and possible waverider geometries that can be developed therefrom are discussed.

TABLE OF CONTENTS

<u>Section</u>	<u>Page</u>
1. Introduction.....	1
2. Governing Equations and Boundary Conditions.....	3
3. Linearization About Circular Cone at Zero Angles of Attack and Yaw.....	13
4. Weak Polar Crossflow Approximation.....	21
5. Hypersonic Small Disturbance Approximation; Comparison with Experiment.....	26
6. Streamsurfaces and Waverider Geometries	45
7. Concluding Remarks.....	54

ACKNOWLEDGEMENTS

REFERENCES

LIST OF FIGURES

<u>Figure</u>		<u>Page</u>
1.	Spherical Polar Coordinate System.....	5
2.	Geometry of Shock and Body.....	7
3.	Spherical Projection of Shock and Body.....	14
4.	Relation Between Shock and Body Shapes ($K_b = M_1 \theta_{ob}$)....	32
5.	Surface Pressure Coefficient ($K_b = M_1 \theta_{ob}$).....	36
6.	Circular Cone at Angle of Attack. Comparison of Theory and Experiment.....	37
7.	Elliptic Cone. Comparison of Theory and Experiment (Case 1, Ref.11).....	40
8.	Elliptic Cone. Comparison of Theory and Experiment (Case 2, Ref.11).....	41
9.	Elliptic Cone. Comparison of Theory and Experiment (Case 3, Ref.11).....	42
10.	Elliptic Cone. Comparison of Theory and Experiment (Case 4, Ref.11).....	43
11.	Crossflow Streamlines, $\theta_b = \theta_{ob} + \theta_{1b} \cos \phi$	48
12.	Crossflow Streamlines, $\theta_b = \theta_{ob} + \theta_{2b} \cos 2 \phi$	49
13.	Crossflow Streamlines, $\theta_b = \theta_{ob} + \theta_{3b} \cos 3 \phi$	50
14.	Crossflow Streamlines, $\theta_b = \theta_{ob} + \theta_{4b} \cos 4 \phi$	51
15.	Waverider Geometries Derived from Flows Past Conical Bodies that Deviate Slightly from a Right Circular Cone (freehand sketches).....	53

LIST OF TABLES

<u>Table</u>	<u>Page</u>
1. Experimental Conditions of Zakkay and Visich (11).....	39

SECTION 1

INTRODUCTION

Conical bodies refer to shapes that are generated by a semi-infinite line, one end of which is fixed at a point called the vertex of the body. By moving any other point on the line through a closed curve, a conical body is generated. A right circular cone is the most common example of a conical body. Many practically important lifting bodies can be approximated as conical or nearly conical, and thus the study of flows past conical shapes is of interest.

Provided the bow shock wave is attached, the flowfield associated with a uniform supersonic flow past a conical body is also conical. That is, the flowfield is independent of distance along a ray through the vertex. Conical flows have been extremely valuable as building blocks for more complex situations and as guides to the nature of supersonic flow. They provide two of the more important exact solutions for inviscid supersonic flow past bodies (e.g. the wedge and right circular cone).

In this report we wish to study supersonic flow past conical bodies whose cross-sections deviate slightly from that of a right circular cone. In this way, we can study the effects of angle of attack, elliptic eccentricity, and so on. Using a regular perturbation scheme as originally suggested by Ferri, Ness, and Kaplita (1) and later used by Chapkis (2), we seek solutions that differ slightly from a known nonlinear flowfield -- here the supersonic flow past a right circular cone. Rather than solve the perturbation problem

numerically, as did Ferri et al., we shall use an approximate, albeit quite accurate, analytical solution for the right circular cone flow that allows the perturbation problem to be solved analytically in closed form. In contrast to Chapkis' solution, the approximate circular cone solution that is employed herein is considerably more accurate. In this way the accuracy and utility of the results are enhanced.

Here we consider bodies which deviate from a right circular cone by amounts proportional to $\cos n\phi$ and $\sin m\phi$. The cone at small angles of attack corresponds to $n = 1$ and the slightly elliptic cone corresponds to $n = 2$. Superposition of the results for various m, n allow a much larger class of body shape to be studied. In this way, the range of conical bodies for which approximate solutions are available has been generalized considerably.

In what follows, we first derive the governing equations and boundary conditions for these conical flows. Using the "linearized characteristics method" of Ferri et al (1), we then derive the small disturbance equations and the simplified form of the boundary conditions. A "weak polar crossflow" approximate solution to these equations is then obtained. Further results are found using the hypersonic small disturbances approximation. Comparisons of these results with experiment is then given. The streamsurfaces and possible waverider geometries that derive from these streamsurfaces are then discussed. The report ends with some concluding remarks.

SECTION 2

GOVERNING EQUATIONS AND BOUNDARY CONDITIONS

The equations expressing conservation of mass, Newton's second law, and the first law of thermodynamics (in both entropy and total enthalpy form) for an inviscid, adiabatic, steady flow are

$$\nabla \cdot (\rho \vec{V}) = 0 \quad (1)$$

$$\rho \vec{V} \cdot \nabla \vec{V} = -\nabla p \quad (2)$$

$$\vec{V} \cdot \nabla s = 0 \quad (3)$$

$$\vec{V} \cdot \nabla (h + V^2/2) = 0 \quad (4)$$

We shall take the state equations to be of the form

$$p = p (\rho, s) \quad (5)$$

$$h = h (p, \rho) \quad (6)$$

Equation (4) can be integrated to give the result that the total enthalpy $h + V^2 / 2$ is constant along streamlines. As we assume the freestream conditions to be uniform, the total enthalpy is constant everywhere.

If we eliminate the pressure and density from the continuity and momentum equations, we obtain

$$0 = \nabla \cdot \vec{V} - \frac{\vec{V}}{a^2} \cdot (\vec{V} \cdot \nabla \vec{V}) \quad (7)$$

$$\frac{1}{\rho} \left(\frac{\partial \rho}{\partial s} \right)_p \nabla s = \frac{1}{\left(\frac{\partial h}{\partial p} \right)_p} \nabla \left(\frac{v^2}{2} \right) + \left(\left(\frac{\partial h}{\partial p} \right)_p + \frac{1}{a^2} \right) \vec{v} \cdot \nabla \vec{v} \quad (8)$$

It is convenient to adopt a spherical polar coordinate system (r, θ, ϕ) aligned with the basic circular cone with origin at the cone vertex (see Figure 1). In this case, Eqs. (4), (7), and (8) become, assuming conical flow (e.g. $\partial/\partial r = 0$),

$$a^2 = \frac{\gamma-1}{2} (V_M^2 - u^2 - v^2 - w^2) \quad (9)$$

$$0 = u \left(2 - \frac{v^2 + w^2}{a^2} \right) + v \cot \theta + \left(1 - \frac{v^2}{a^2} \right) \frac{\partial v}{\partial \theta} \quad (10)$$

$$+ \left(1 - \frac{w^2}{a^2} \right) \frac{1}{\sin \theta} \frac{\partial w}{\partial \phi} - \frac{vw}{a^2} \left(\frac{1}{\sin \theta} \frac{\partial v}{\partial \phi} + \frac{\partial w}{\partial \theta} \right)$$

$$0 = v \frac{\partial u}{\partial \theta} + \frac{w}{\sin \theta} \frac{\partial u}{\partial \phi} - v^2 - w^2 \quad (11)$$

$$\frac{a^2}{\gamma R} \frac{\partial s}{\partial \theta} = -u \frac{\partial u}{\partial \theta} - w \frac{\partial w}{\partial \theta} + \frac{w}{\sin \theta} \frac{\partial v}{\partial \phi} + uv - w^2 \cot \theta \quad (12)$$

$$\begin{aligned} \frac{a^2}{\gamma R} \frac{\partial s}{\partial \phi} = & -u \frac{\partial u}{\partial \phi} - v \frac{\partial v}{\partial \phi} + v \sin \theta \frac{\partial w}{\partial \theta} + uw \sin \theta \\ & + v w \cos \theta \end{aligned} \quad (13)$$

Here V_M is the maximum attainable velocity for the given total enthalpy h_0 , $V_M = \sqrt{2 h_0}$. Equations (9) - (13) also assume a perfect gas model for which Eqs. (5) and (6) reduce to

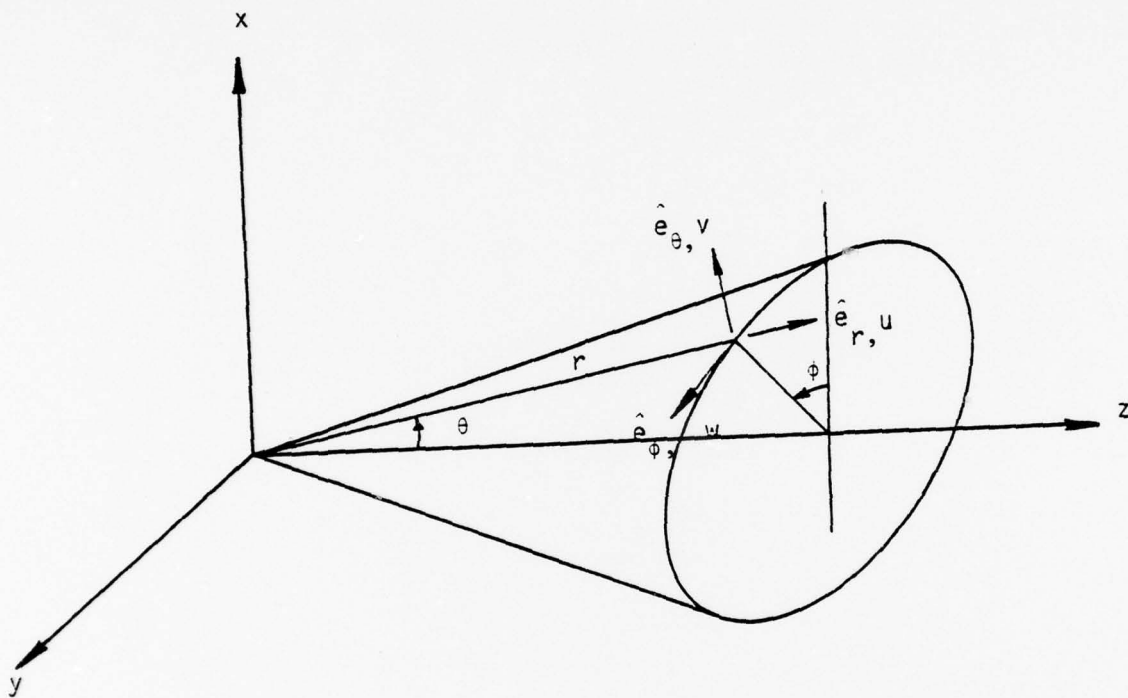


FIGURE 1. SPHERICAL POLAR COORDINATE SYSTEM

$$p = p_1 \left(\frac{\rho}{\rho_1} \right)^\gamma \exp \left(\frac{s-s_1}{c_v} \right) \quad (14)$$

$$h = \frac{\gamma}{\gamma-1} \frac{p}{\rho} \quad (15)$$

The subscript 1 refers to a reference state taken here to be the undisturbed freestream conditions.

The boundary conditions for this problem include the shock jump relations and the condition of zero mass flux through the body -- the so-called tangency condition. The shock jump conditions can be written

$$\rho_1 \vec{V}_1 \cdot \hat{n}_s = \rho_2 \vec{V}_2 \cdot \hat{n}_s = m \quad (16)$$

$$m \vec{V}_1 + p_1 \hat{n}_s = m \vec{V}_2 + p_2 \hat{n}_s \quad (17)$$

$$m \left(h_1 + \frac{V_1^2}{2} \right) = m \left(h_2 + \frac{V_2^2}{2} \right) \quad (18)$$

Here the subscripts 1 and 2 refer to conditions upstream and downstream of the shock wave and \hat{n}_s is the unit normal to the shock (see Figure 2). The freestream conditions are taken to be constant with velocity \vec{V}_1 at angle of attack α and angle of yaw τ relative to the z - axis,

$$\vec{V}_1 = \frac{V_1}{(1 + \tan^2 \alpha + \tan^2 \tau)^{1/2}} (\hat{e}_z + \tan \alpha \hat{e}_x + \tan \tau \hat{e}_y) \quad (19)$$

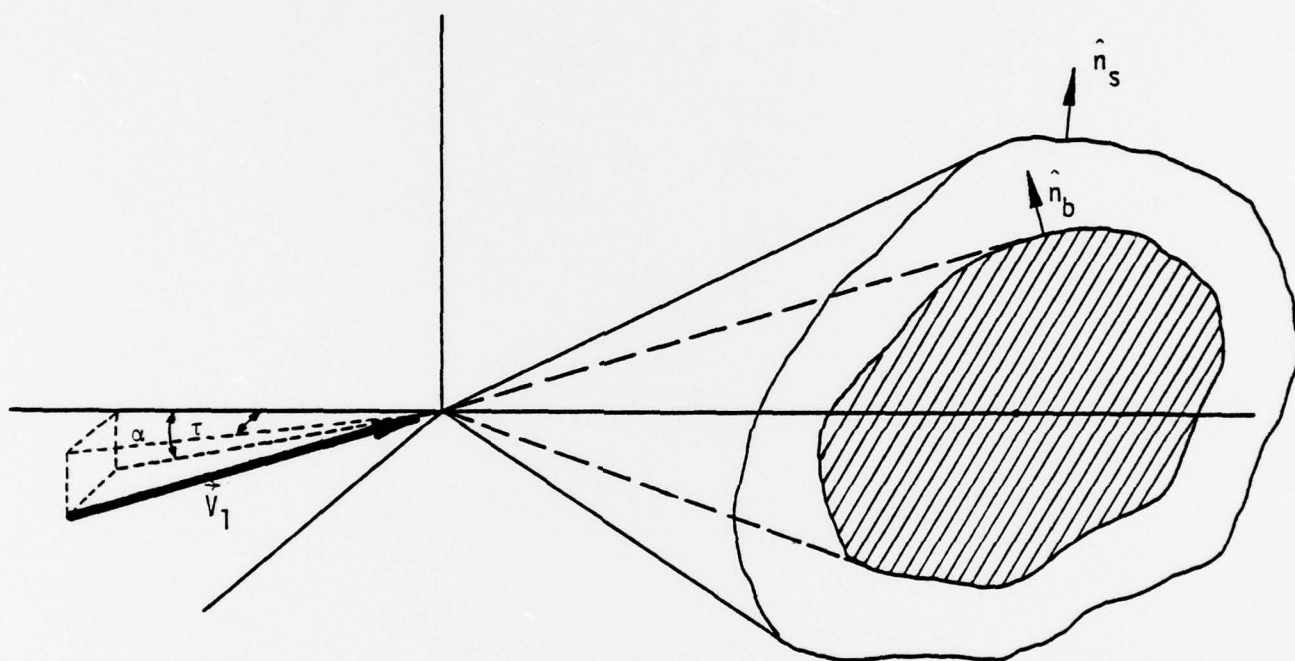


FIGURE 2. GEOMETRY OF SHOCK AND BODY

The tangency condition on the body can be written

$$\vec{V} \cdot \hat{n}_b = 0 \quad \text{on body} \quad (20)$$

Here \hat{n}_b is the unit normal to the body.

The component of the freestream Mach number normal to the shock wave, M_{1n} , is given by

$$M_{1n} = \vec{M}_1 \cdot \hat{n}_s ; \quad \vec{M}_1 = \frac{\vec{V}_1}{a_1} \quad (21)$$

For a calorically perfect gas, the shock jump conditions can be rewritten

$$\frac{\vec{V}_1 \cdot \hat{n}_s}{\vec{V}_2 \cdot \hat{n}_s} = \frac{\rho_2}{\rho_1} = \frac{(\gamma+1) M_{1n}^2}{(\gamma-1) M_{1n}^2 + 2} \quad (22)$$

$$\vec{V}_1 \times \hat{n}_s = \vec{V}_2 \times \hat{n}_s \quad (23)$$

$$\frac{p_2}{p_1} = 1 + \frac{2\gamma}{\gamma+1} (M_{1n}^2 - 1) \quad (24)$$

$$\frac{\Delta S}{c_v} = \ln \left[\left(\frac{2\gamma M_{1n}^2 - (\gamma-1)}{\gamma+1} \right)^{\gamma} \left(-\frac{(\gamma-1) M_{1n}^2 + 2}{(\gamma+1) M_{1n}^2} \right) \right] \quad (25)$$

For conical flows, we can take the equations describing the shock wave and body as

$$\text{shock wave:} \quad \theta = \theta_s (\phi) \quad (26)$$

$$\text{body:} \quad \theta = \theta_b (\phi) \quad (27)$$

In the direct problem that we are considering, $\theta_b(\phi)$ is given and $\theta_s(\phi)$ is to be determined. We introduce the angles β and δ so that

$$\hat{n}_s = \cos \beta \hat{e}_\theta - \sin \beta \hat{e}_\phi \quad (28)$$

$$\hat{n}_b = \cos \delta \hat{e}_\theta - \sin \delta \hat{e}_\phi \quad (29)$$

where

$$\tan \beta = \frac{1}{\sin \theta_s} \frac{d\theta_s}{d\phi}, \quad \tan \delta = \frac{1}{\sin \theta_b} \frac{d\theta_b}{d\phi} \quad (30)$$

The expression for the normal component of the freestream Mach number can then be rewritten (31)

$$M_{1n} = \frac{M_1}{(1 + \tan^2 \alpha + \tan^2 \tau)^{1/2}} [\cos \beta (-\sin \theta + \tan \alpha \cos \theta \cos \phi + \tan \tau \cos \theta \sin \phi) - \sin \beta (-\tan \alpha \sin \phi + \tan \tau \cos \phi)]$$

Equations (22) and (23) can be solved for the three velocity components downstream of the shock wave in the following form

$$\frac{u_2}{V_1} = \frac{1}{(1 + \tan^2 \alpha + \tan^2 \tau)^{1/2}} [\cos \theta + \tan \alpha \sin \theta \cos \phi + \tan \tau \sin \theta \sin \phi] \quad (32)$$

(33)

$$\frac{v_2}{V_1} = \frac{1}{(1 + \tan^2 \alpha + \tan^2 \tau)^{1/2}} [\cos \beta \{ \cos \beta (-\sin \theta + \tan \alpha \cos \theta \cos \phi + \tan \tau \cos \theta \sin \phi) - \sin \beta (-\tan \alpha \sin \phi + \tan \tau \cos \phi) \}$$

$$\cdot \left\{ \frac{\gamma-1}{\gamma+1} + \frac{2}{(\gamma+1) M_{1n}^2} \right\}$$

$$- \sin \beta \{ -\cos \beta (-\tan \alpha \sin \phi + \tan \tau \cos \phi) - \sin \beta (-\sin \theta + \tan \alpha \cos \theta \cos \phi + \tan \tau \cos \theta \sin \phi) \}]$$

$$\begin{aligned}
\frac{w}{V_1} = & \frac{1}{(1 + \tan^2 \alpha + \tan^2 \tau)^{1/2}} [- \sin \beta \{ \cos \beta (- \sin \theta \\
& + \tan \alpha \cos \theta \cos \phi + \tan \tau \cos \theta \sin \phi) \\
& - \sin \beta (- \tan \alpha \sin \phi + \tan \tau \cos \phi) \} \\
& \cdot \{ \frac{\gamma-1}{\gamma+1} + \frac{2}{(\gamma+1) M_{1n}^2} \} \\
& - \cos \beta \{ - \cos \beta (- \tan \alpha \sin \phi + \tan \tau \cos \phi) \\
& - \sin \beta (- \sin \theta + \tan \alpha \cos \theta \cos \phi + \tan \tau \cos \theta \sin \phi) \}] \quad (34)
\end{aligned}$$

Here θ is to be evaluated at $\theta_s(\phi)$. The tangency condition on the body becomes

$$0 = v_2 \cos \delta - w_2 \sin \delta \quad (35)$$

with θ evaluated at $\theta_b(\phi)$.

Equations (10) - (13) give four nonlinear partial differential equations for the four unknowns u , v , w , and s . Equations (25) and (32) - (35) give five boundary conditions. Thus the unknown shock shape $\theta_s(\phi)$ can also be determined. Once the velocity and entropy are known, the pressure coefficient, C_p ,

$$C_p = \frac{p - p_1}{\frac{1}{2} \rho_1 V_1^2} \quad (36)$$

can be determined from

$$C_p = \frac{2}{\gamma M_1^2} \left\{ \left(\frac{V_M^2 - V^2}{V_M^2 - V_1^2} \right)^{\frac{\gamma}{\gamma-1}} \exp \left(- \frac{s - s_1}{R} \right) - 1 \right\} \quad (37)$$

It is convenient to introduce the following normalized variables,

$$\bar{V}_1 = \frac{V_1}{V_1}, \quad \bar{p} = \frac{p}{\rho_1 V_1^2}, \quad \bar{s} = \frac{s - s_1}{c_v}, \quad \bar{\rho} = \frac{\rho}{\rho_1}, \quad \bar{a} = \frac{a}{V_1} \quad (38)$$

Dropping the bars for convenience, we can then rewrite Eqs. (10) - (13) as,

$$C = u \left(2 - \frac{v^2 + w^2}{a^2} \right) + v \cot \theta + \left(1 - \frac{v^2}{a^2} \right) \frac{\partial v}{\partial \theta} + \left(1 - \frac{w^2}{a^2} \right) \cdot \frac{1}{\sin \theta} \frac{\partial w}{\partial \phi} - \frac{vw}{a^2} \left(\frac{1}{\sin \theta} \frac{\partial v}{\partial \phi} + \frac{\partial w}{\partial \theta} \right) \quad (39)$$

$$0 = v \frac{\partial u}{\partial \theta} + \frac{w}{\sin \theta} \frac{\partial u}{\partial \phi} - v^2 - w^2 \quad (40)$$

$$\frac{a^2}{\gamma(\gamma-1)} \frac{\partial s}{\partial \theta} = -u \frac{\partial u}{\partial \theta} - w \frac{\partial w}{\partial \theta} + \frac{w}{\sin \theta} \frac{\partial v}{\partial \phi} + uv - w^2 \cot \theta \quad (41)$$

$$\frac{a^2}{\gamma(\gamma-1)} \frac{\partial s}{\partial \phi} = -u \frac{\partial u}{\partial \phi} - v \frac{\partial v}{\partial \phi} + v \sin \theta \frac{\partial w}{\partial \theta} + uw \sin \theta + vw \cos \theta \quad (42)$$

where a^2 is given by

$$a^2 = \frac{\gamma-1}{2} (V_M^2 - V^2), \quad V_M^2 = 1 + \frac{2}{(\gamma-1) M_1^2} \quad (43)$$

The boundary conditions on the velocity are still given in Eqs. (32)-(35) with the left-hand-side of Eqs. (32) - (34) replaced by u , v , and w ,

respectively. The boundary condition on the entropy s becomes

$$s = \ln \left\{ \left(\frac{2\gamma M_1^2 (\gamma-1)}{\gamma+1} \right)^{\frac{\gamma}{2}} \left(\frac{(\gamma-1) M_1^2}{(\gamma+1) M_1^2} \right)^{\frac{\gamma}{2}} \right\} \text{ at } \theta = \theta_s \quad (44)$$

while the expression for the pressure coefficient C_p becomes

$$C_p = \frac{2}{\gamma M_1^2} \left\{ \left(\frac{V_M^2 - V^2}{V_M^2 - 1} \right)^{\frac{\gamma}{\gamma-1}} \exp \left(- \frac{s}{\gamma-1} \right) - 1 \right\} \quad (45)$$

SECTION 3

LINEARIZATION ABOUT CIRCULAR CONE AT ZERO ANGLES OF ATTACK AND YAW.

Let us assume that the flowfield is conical and deviates slightly from that for flow past a right circular cone at zero angles of attack and yaw (see Figure 3). Furthermore, let us expand the flowfield variables in a Fourier series in the azimuthal angle ϕ .

$$\begin{aligned}
 u &= u_0 + \sum_{n=1}^{\infty} \theta_{n_b} u_n(\theta) \cos n\phi + \sum_{m=1}^{\infty} \theta_{m_b} u_m(\theta) \sin m\phi \\
 v &= v_0 + \sum_{n=1}^{\infty} \theta_{n_b} v_n(\theta) \cos n\phi + \sum_{m=1}^{\infty} \theta_{m_b} v_m(\theta) \sin m\phi \\
 w &= \sum_{n=1}^{\infty} \theta_{n_b} w_n(\theta) n \sin n\phi - \sum_{m=1}^{\infty} \theta_{m_b} w_m(\theta) m \cos m\phi \\
 s &= s_0 + \sum_{n=1}^{\infty} \theta_{n_b} s_n(\theta) \cos n\phi + \sum_{m=1}^{\infty} \theta_{m_b} s_m(\theta) \sin m\phi \\
 \theta_s &= \theta_{0_s} + \sum_{n=1}^{\infty} \theta_{n_s} \cos n\phi + \sum_{m=1}^{\infty} \theta_{m_s} \sin m\phi \\
 \theta_b &= \theta_{0_b} + \sum_{n=1}^{\infty} \theta_{n_b} \cos n\phi + \sum_{m=1}^{\infty} \theta_{m_b} \sin m\phi
 \end{aligned} \tag{46}$$

The subscript naught refers to the basic flow past a right circular cone at zero angles of attack and yaw. In order that the flowfield deviate slightly from this basic flow, the Fourier coefficients θ_{n_b} and θ_{m_b} (and

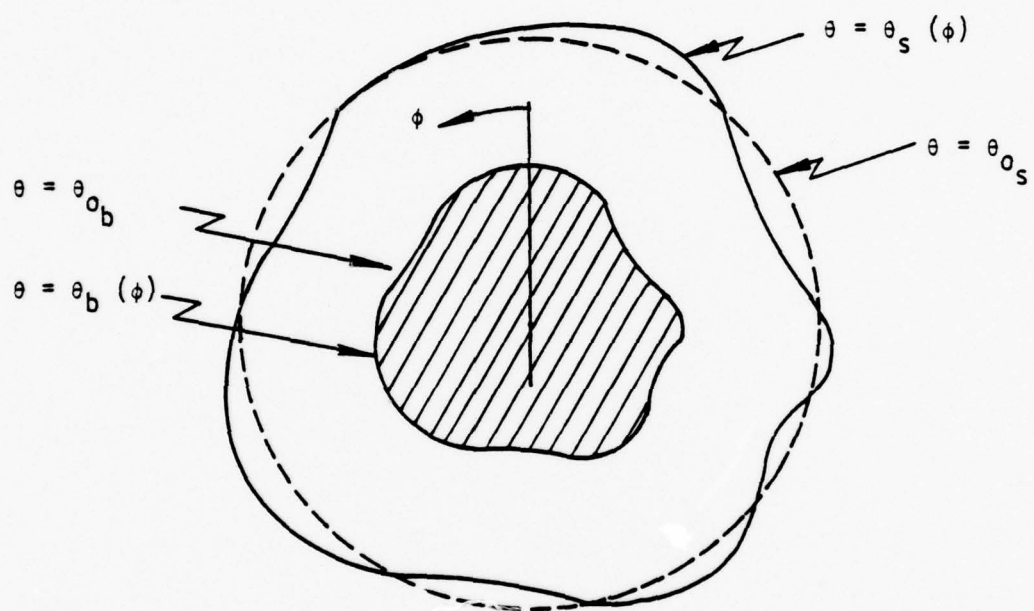


FIGURE 3. SPHERICAL PROJECTION OF SHOCK AND BODY

therefore θ_{n_s} and θ_{m_s} must be small compared to θ_{o_b} (and θ_{o_s}),

$$\frac{\theta_{n_c}}{\theta_{o_b}}, \quad \frac{\theta_{m_c}}{\theta_{o_b}} \ll 1$$

(47)

$$\frac{\theta_{n_s}}{\theta_{o_s}}, \quad \frac{\theta_{m_s}}{\theta_{o_s}} \ll 1$$

We shall assume this is true so that terms of second order in θ_{n_b} and θ_{n_s} are negligible. For consistency, we also assume the angles of attack α and yaw τ are similarly small compared to θ_{o_b} .

Substituting these expansions into the governing equations and boundary condition, and equating coefficients of powers of θ_{n_b} , θ_{m_b} to zero, we obtain a hierarchy of problems, the first being that for flow past a right circular cone at zero angles of attack and yaw. The governing equations for that problem are

$$2 u_o + \cot \theta v_o + \frac{dv_o}{d\theta} = \left(\frac{v_o}{a_o}\right)^2 \left(u_o + \frac{dv_o}{d\theta}\right) \quad (48)$$

$$0 = v_o \frac{du_o}{d\theta} - v_o^2 \quad (49)$$

$$\frac{a_o^2}{\gamma(\gamma-1)} \frac{ds_o}{d\theta} = -u_o \frac{du_o}{d\theta} + u_o v_o \quad (50)$$

with

$$a_o^2 = \frac{-1}{2} (V_M^2 - a_o^2 - v_o^2) \quad (51)$$

The associated boundary conditions are

$$\theta = \theta_{o_s} :$$

$$\begin{aligned}
u_0 &= \cos \theta \\
v_0 &= -\frac{\gamma-1}{\gamma+1} \left(\frac{v_M^2 - \cos^2 \theta}{\sin \theta} \right) \\
s_0 &= \ln \left[\left(-\frac{2\gamma M_1^2 \sin^2 \theta - \gamma + 1}{\gamma + 1} \right) \left(-\frac{(\gamma-1)M_1^2 \sin^2 \theta + 2}{\gamma + 1} \right)^{\frac{\gamma}{\gamma-1}} \right]
\end{aligned} \tag{52}$$

$$\begin{aligned}
\theta &= \theta_{0b} : \\
v_0 &= 0
\end{aligned} \tag{53}$$

The equations for the first order (e.g. of order θ_{nb} , θ_{mb}) problem are

$$\begin{aligned}
2 u_n + \cot \theta v_n + \frac{dv_n}{d\theta} + \frac{n^2 w_n}{\sin \theta} \\
= \left(\frac{v_0}{a_0} \right)^2 \left[u_n - 2 u_0 \frac{a_n}{a_0} + \frac{dv_n}{d\theta} - 2 \frac{a_n}{a_0} \frac{dv_0}{d\theta} \right. \\
\left. + 2 v_n \frac{d \ln v_0}{d\theta} \right] + \left(\frac{v_0}{a_0} \right) \left[2 \frac{u_0}{a_0} v_n \right]
\end{aligned} \tag{54}$$

$$0 = v_0 \frac{du_n}{d\theta} + v_n \frac{du_0}{d\theta} - 2 v_0 v_n \tag{55}$$

$$-\frac{a_0^2}{\gamma(\gamma-1)} \frac{ds_n}{d\theta} = u_0 \left(v_n - \frac{du_n}{d\theta} \right) \tag{56}$$

$$\begin{aligned}
-\frac{a_0^2}{\gamma(\gamma-1)} s_n &= u_0 u_n + v_0 v_n + v_0 \sin \theta \frac{dw_n}{d\theta} \\
&+ w_n (u_0 \sin \theta + v_0 \cos \theta)
\end{aligned} \tag{57}$$

$$0 = \frac{a_n}{a_0} + \frac{\gamma-1}{2} \left(\frac{u_0}{a_0} \frac{u_n}{a_0} + \frac{v_0}{a_0} \frac{u_n}{a_0} \right) \tag{58}$$

The associated boundary conditions are

$$\theta = \theta_{0s} :$$

$$\begin{aligned} u_n &= (-\sin \theta - \frac{du_0}{d\theta} + \lambda \delta_{1n} \sin \theta) \frac{\theta_{ns}}{\theta_{nb}} \\ v_n &= \left(-\frac{dv_0}{d\theta} - v_0 \cot \theta \frac{2 - (\gamma-1) M_1^2 \sin^2 \theta}{2 + (\gamma-1) M_1^2 \sin^2 \theta} \right. \\ &\quad \left. \cdot (1 - \lambda \delta_{1n}) \right) \frac{\theta_{ns}}{\theta_{nb}} \\ w_n &= \left(\frac{2}{\gamma+1} \left(1 - \frac{1}{M_1^2 \sin^2 \theta} \right) - \lambda \delta_{1n} \right) \frac{\theta_{ns}}{\theta_{nb}} \\ s_n &= \left(-\frac{ds_0}{d\theta} + \frac{4 \gamma (\gamma-1) \cot \theta (M_1^2 \sin^2 \theta - 1)^2}{(2 \gamma M_1^2 \sin^2 \theta - \gamma + 1) ((\gamma-1) M_1^2 \sin^2 \theta + 2)} \right. \\ &\quad \left. \cdot (1 - \lambda \delta_{1n}) \right) \frac{\theta_{ns}}{\theta_{nb}} \end{aligned} \quad (59)$$

$$\theta = \theta_{0b}$$

$$v_n = 2 u_0 \quad (60)$$

Here λ is $(\tan \alpha) / \theta_{1s}$ or $(\tan \tau) / \theta_{1s}$ for cases involving angle of attack ($n=1$) or yaw ($m=1$). δ_{1n} is the Kronecker delta symbol.

Equations (55) and (56) can be used to show that s_n is constant and that v_n equals $du_n / d\theta$. The result that s_n is constant is not valid on the body surface. The body surface is a streamsurface and the entropy must be constant there. Our perturbation approach gives $s = s_0 + \sum s_n \cos n \phi + \sum s_m \sin m \phi$ which is not constant on the body surface. As a consequence there is a thin layer near the body surface, the so-called

vortical layer, where the results of our regular perturbation scheme are not valid. Munson (5), Melnik (6), and others have studied conditions in the vortical layer and have shown that the results obtained for the pressure and azimuthal velocity by means of the regular perturbation approach are valid in the vortical layer while the results for the radial and polar velocities and entropy are not valid there. The methods of singular perturbation theory allow one to correct the inadequacies of the regular perturbation approach near the body and thereby obtain a uniformly valid solution. We shall not attempt to deal with the vortical layer as it will not affect the results of interest to us.

Equation (57) can now be rewritten

$$-\frac{a_0^2}{\gamma(\gamma-1)v_0} s_n = \frac{d}{d\theta} (u_n + w_n \sin \theta) + \frac{u_0}{v_0} (u_n + w_n \sin \theta) \quad (61)$$

which can be formally integrated to give

$$\begin{aligned} u_n + w_n \sin \theta &= -\frac{s_n}{\gamma(\gamma-1)} (-v_0 \sin \theta)^{1/2} \frac{1}{a_0^{\gamma-1}} \\ &\quad \cdot \int_{\theta_{0s}}^{\theta} \frac{a_0^{\frac{2\gamma-3}{\gamma-1}}}{v_0 (-v_0 \sin \theta)^{1/2}} d\theta \\ &= -F_n(\theta) \end{aligned} \quad (62)$$

noting that $(u_n + w_n \sin \theta)$ vanishes at $\theta = \theta_{0s}$. Eliminating v_n and w_n from Eq. (54), we obtain

$$\frac{d^2 u_n}{d\theta^2} + \cot \theta \frac{du_n}{d\theta} + u_n (2 - n^2 \csc^2 \theta) = \frac{n^2 F_n(\theta)}{\sin^2 \theta} \quad (63)$$

$$+ 2 \frac{v_0}{a_0} \frac{u_0}{a_0} \frac{du_n}{d\theta} + \left(\frac{v_0}{a_0}\right)^2 \left[u_n + \frac{d^2 u_n}{d\theta^2} - 2 \left(u_0 + \frac{dv_0}{d\theta} \right) \frac{a_n}{a_0} + 2 \frac{v_n}{v_0} \frac{dv_0}{d\theta} \right]$$

with boundary conditions

$$\begin{aligned} \theta = \theta_{0s} : \quad u_n &= - \left[\frac{du_0}{d\theta} + \sin \theta (1 - \lambda \delta_{1n}) \right] \frac{\theta_{ns}}{\theta_{nb}} \\ \frac{du_n}{d\theta} &= - \left[\frac{dv_0}{d\theta} + v_0 \cot \theta \left(\frac{2 - (\gamma - 1) M_1^2 \sin^2 \theta}{2 + (\gamma - 1) M_1^2 \sin^2 \theta} \right) \right. \\ &\quad \left. \cdot (1 - \lambda \delta_{1n}) \right] \frac{\theta_{ns}}{\theta_{nb}} \end{aligned} \quad (64)$$

$$\theta = \theta_{0b} : \quad \frac{du_n}{d\theta} = 2 u_0 \quad (65)$$

Once u_n is determined, w_n follows from Eq. (62) and v_n follows from

$$v_n = \frac{du_n}{d\theta} \quad (66)$$

The disturbance sound speed a_n can be evaluated from Eq. (58). The constant s_n is given by Eq. (59).

The pressure coefficient C_p can also be expressed as a Fourier series expansion. Substituting for V and s in Eq. (45), we obtain

$$C_p = C_{p_0} + \sum_{n=1}^{\infty} \theta_{nb} C_{pn}(\theta) \cos n\phi + \sum_{m=1}^{\infty} \theta_{mb} C_{pm}(\theta) \sin m\phi \quad (67)$$

where

$$C_{p_o} = \frac{2}{\gamma M_1^2} \left\{ \left(\frac{V_M^2 - u_o^2 - v_o^2}{V_M^2 - 1} \right)^{\frac{\gamma}{\gamma-1}} \exp \left(\frac{-s_o}{\gamma-1} \right) - 1 \right\} \quad (68)$$

$$C_{p_n} = - \left(C_{p_o} + \frac{2}{\gamma M_1^2} \right) \left\{ \frac{s_n}{\gamma-1} + \frac{2\gamma}{\gamma-1} \frac{u_o u_n + v_o v_n}{V_M^2 - u_o^2 - v_o^2} \right\} \quad (69)$$

SECTION 4

WEAK POLAR CROSSFLOW APPROXIMATION

Here we wish to exploit an approximation introduced earlier by Rasmussen (7) that allows closed-form analytical results to be obtained. These approximate results are surprisingly accurate over a wide range of conditions and are particularly simple to use. The approximation we shall invoke is the "weak polar crossflow approximation" corresponding to the limit $v_o/a_o \rightarrow 0$. The term $(v_o/a_o)^2$ varies from its maximum value at the shock to zero on the body,

$$0 \leq \left(\frac{v_o}{a_o}\right)^2 \leq \left(\frac{v_o}{a_o}\right)^2_{\text{shock}} = \frac{(\gamma-1) M_1^2 \sin^2 \theta + 2}{2\gamma M_1^2 \sin^2 \theta - \gamma + 1} \quad (70)$$

For $M_1 \sin \theta$ large, the upper bound to $(v_o/a_o)^2$ becomes $(\gamma-1) / 2\gamma$ ($= 1/7$ if $\gamma = 1.4$). As we shall see, ignoring terms of order v_o/a_o in the governing equations reduces the equations to forms that can be solved analytically in terms of known functions.

Ignoring terms of order $(v_o/a_o)^2$ in Eq. (48), we can reduce the equations governing flow past a right circular cone at zero angles of attack and yaw, Eqs. (48) - (51), to

$$\frac{d^2 u_o}{d\theta^2} + \cot \theta \frac{du_o}{d\theta} + 2 u_o = 0 \quad (71)$$

$$v_o = \frac{du_o}{d\theta} \quad (72)$$

$$a_o^2 = \frac{\gamma-1}{2} (V_M^2 - u_o^2 - v_o^2) \quad (73)$$

$$s_0 = \ln \left\{ \left(\frac{2\gamma M_1^2 \sin^2 \theta_{0s} - \gamma + 1}{(\gamma + 1)} \right) \left(\frac{(\gamma - 1) M_1^2 \sin^2 \theta_{0s} + 2}{(\gamma + 1) M_1^2 \sin^2 \theta_{0s}} \right)^\gamma \right\} \quad (74)$$

with boundary conditions

$$\begin{aligned} \theta = \theta_{0s} : \quad u_0 &= \cos \theta \\ \frac{du_0}{d\theta} &= - \frac{\gamma - 1}{\gamma + 1} \left(\frac{V_M^2 - \cos^2 \theta}{\sin \theta} \right) \end{aligned} \quad (75)$$

$$\theta = \theta_{0b} : \quad \frac{du_0}{d\theta} = 0 \quad (76)$$

Equation (71) is Legendre's equation whose solution can be written

$$u_0 = A_0 P_1(\mu) + B_0 Q_1(\mu) \quad (77)$$

($\mu = \cos \theta$). Here P_n and Q_n are the Legendre functions of the first and second kind, respectively. In particular,

$$P_1(\mu) = \mu, \quad Q_1(\mu) = \frac{\mu}{2} \ln \left(\frac{1+\mu}{1-\mu} \right) - 1 \quad (78)$$

The boundary conditions, Eqs. (75), allow the constants A_0 and B_0 to be evaluated. The results are

$$\begin{aligned} A_0 &= 1 + \left[(1-\mu^2) Q_1(\mu) \left(1 - \frac{\gamma-1}{\gamma+1} \frac{V_M^2 - \mu^2}{1-\mu^2} \right) \right]_{\mu=\mu_s} \\ B_0 &= - \left[\mu(1-\mu^2) \left(1 - \frac{\gamma-1}{\gamma+1} \frac{V_M^2 - \mu^2}{1+\mu^2} \right) \right]_{\mu=\mu_s} \end{aligned} \quad (79)$$

Here $\mu_s = \cos \theta_{0s}$. The cone angle θ_{0b} ($= \cos^{-1} \mu_b$) follows from

$$\left(\frac{dQ_1}{d\mu} \right)_{\mu=\mu_b} = \left\{ \frac{\frac{dQ_1}{d\mu} - \frac{\gamma-1}{\gamma+1} \frac{V_M^2 - \mu^2}{1-\mu^2} Q_1}{1 - \frac{\gamma-1}{\gamma+1} \frac{V_M^2 - \mu^2}{1-\mu^2}} \right\}_{\mu=\mu_s} \quad (80)$$

We now wish to apply this weak crossflow approximation to the perturbation problem, Eq. (63). Equation (63) contains terms on the right-hand side that are order $(u_0/a_0) (v_0/a_0)$ and $(v_0/a_0)^2$ relative to terms on the left-hand side. The terms of order $(v_0/a_0)^2$ on the right-hand side are uniformly small compared to like terms retained on the left-hand side in this weak polar crossflow approximation. This is not the case, however, for the term of order $(u_0 v_0/a_0^2)$. Specifically, if we compare the term $2 (u_0/a_0) (v_0/a_0) du_0/d\theta$ on the right-hand side with the term $\cot\theta du_n/d\theta$ on the left-hand side, we see that their ratio varies from a maximum at the shock to zero on the body. The value of the ratio at the shock is given by

(81)

$$\left[\frac{2}{\cot\theta} \left(\frac{u_0}{a_0} \right) \left(\frac{v_0}{a_0} \right) \right]_{\theta=\theta_s} = \frac{-4}{(\gamma+1) \left[1 - \frac{(\gamma-1)}{\gamma+1} \right]^2 \left(1 + \frac{2}{(\gamma+1) M_1^2 \sin^2 \theta_s} \right)}$$

which is not small compared to unity. Nonetheless, we shall ignore the term $2(u_0/a_0) (v_0/a_0)$ on the right-hand side for the following reasons. First, this term is relatively important only near the shock. On the body it is identically zero. Second, although the resulting governing equation is somewhat inaccurate near the shock, the solution u_n is still required to satisfy exactly the boundary conditions given by Eqs. (64). As we shall see, the results obtained by ignoring this term compared well with experiment and other more accurate numerical solutions.

Thus, in the weak crossflow limit, Eq. (63) reduces to

$$\frac{d^2 u_n}{d\theta^2} + \cot\theta \frac{du_n}{d\theta} + (2 - n^2 \csc^2 \theta) u_n = n^2 \csc^2 \theta F_n(\theta) \quad (82)$$

The boundary conditions remain unchanged and are given by Eqs. (64, 65). Equation (82) is formally the nonhomogeneous associated Legendre equation of order one and degree n . If we note that $Q_1^n(\theta)$ is a solution of the homogeneous equation^{*}, where

$$Q_1^n = (-1)^n (1-\mu^2)^{n/2} \frac{d^n Q_1}{d\mu^n}, \quad \mu = \cos\theta \quad (83)$$

then the method of variation of parameters gives the solution of (82) as

$$\begin{aligned} u_n(\theta) = & n^2 Q_1^n(\theta) \int_{\theta}^{\theta_{0s}} \frac{d\theta'}{Q_1^{n-2}(\theta') \sin \theta'} \int_{\theta'}^{\theta_{0s}} F_n(\theta'') \cos \theta'' \\ & \cdot Q_1^n(\cos \theta'') d\theta'' + A_n Q_1^n(\theta) \int_{\theta}^{\theta_{0s}} \frac{d\theta'}{Q_1^{n-2}(\theta') \sin \theta'} \\ & + B_n Q_1^n(\theta) \end{aligned} \quad (84)$$

The boundary conditions, Eq. (64), allow the constants A_n and B_n to be evaluated as

^{*}The function $\sin\theta$ is also a complementary solution for the case $n = 1$.

$$A_n = \left[\sin \theta \frac{dQ_1^n}{d\theta} u_n - \sin \theta Q_1^n \frac{du_n}{d\theta} \right]_{\theta=\theta_{0s}} \quad (85)$$

$$B_n = \left[\frac{u_n}{Q_1^n} \right]_{\theta=\theta_{0s}} \quad (86)$$

Equation (65) allows one to determine the ratio of the shock displacement θ_{n_s} to the body perturbation θ_{n_b} .

The integrations required to evaluate Eq. (84) for $u_n(\theta)$ cannot be carried out in closed form. For this reason it is useful to consider a further approximation and restrict attention to slender bodies. In this way, explicit results can be obtained which are quite useful.

SECTION 5

HYPERSONIC SMALL DISTURBANCE APPROXIMATION; COMPARISON WITH EXPERIMENT

Here we wish to consider slender bodies for which, $\theta_s, \theta_b \rightarrow 0$. In order to retain the essentially nonlinear character of supersonic-hypersonic flow, we shall also require M_1 to be large so that

$$K = M_1 \sin \theta \quad (87)$$

is finite. The limit $\theta \rightarrow 0, M \rightarrow \infty$ such that $K_\theta = M_1 \sin \theta$ is finite is the hypersonic small disturbance approximation limit.

In the hypersonic small disturbance approximation, the solution for flow past a right circular cone at zero angles of attack and yaw reduces to (3)

$$u_o = 1 - \frac{1}{2} \sin^2 \theta_b \left[\left(\frac{K_\theta}{K_b} \right)^2 + \ln \left(\frac{K_s}{K_\theta} \right)^2 \right] \quad (88)$$

$$v_o = - \sin \theta \left[1 - \left(\frac{K_b}{K_\theta} \right)^2 \right] \quad (89)$$

$$a_o^2 = \frac{1}{M_1^2} \left[1 + \frac{\gamma-1}{2} K_b^2 \left(2 + \ln \left(\frac{K_s}{K_\theta} \right)^2 - \left(\frac{K_b}{K_\theta} \right)^2 \right) \right] \quad (90)$$

where $K_s = M_1 \sin \theta_{o_s}$ and $K_b = M_1 \sin \theta_{o_b}$. In Eqs. (88-90) we have written θ_b for θ_{o_b} and θ_s for θ_{o_s} to simplify the notation. We shall follow this practice hereafter. The shock angle θ_s and cone angle θ_b are related by

$$\frac{\theta_s}{\theta_b} = \left(\frac{\gamma+1}{2} + \frac{1}{K_b^2} \right)^{1/2} \quad (91)$$

These results allow one to evaluate the function $F_n(\theta)$ that appears in Eq. (62). Ignoring the variation of a_0 across the shock layer in comparison with the variation of v_0 , we obtain

$$F_n = \theta_s G \left[1 - \left(\frac{K_\theta^2 - K_b^2}{K_s^2 - K_b^2} \right)^{1/2} \right] \quad (92)$$

where

$$G = \frac{s_n a_0^2}{\theta_s \gamma (\gamma - 1)} \quad (93)$$

$$= \frac{(K_s^2 - 1)^2}{K_s^2 (2\gamma K_s^2 - \gamma + 1) ((\gamma - 1) K_s^2 + 2)} \left(1 + \frac{\gamma - 1}{2} K_b^2 \left(2 - \frac{K_b^2}{K_s^2} \right) \right)$$

Here $K_s = M_1 \theta_s$ and $K_b = M_1 \theta_b$.

In this hypersonic small disturbance theory limit, Eq. (82) becomes

$$\frac{d^2 u_n}{d\theta^2} + \frac{1}{\theta} \frac{d u_n}{d\theta} - \frac{n^2}{\theta^2} u_n = \frac{n^2}{\theta^2} F_n(\theta) \quad (94)$$

with boundary conditions

$$\theta = \theta_s : \quad u_n = \frac{\theta_{n_s}}{\theta_{n_b}} \theta_s \left(- \frac{\theta_b^2}{\theta_s^2} + \lambda \delta_{1n} \right)$$

$$\frac{d u_n}{d\theta} = \frac{\theta_{n_s}}{\theta_{n_b}} \left(1 + \frac{\theta_b^2}{\theta_s^2} + \left(1 - \frac{\theta_b^2}{\theta_s^2} \right) \frac{2 - (\gamma - 1) K_s^2}{2 + (\gamma - 1) K_s^2} \right. \quad (95)$$

$$\left. \cdot (1 - \lambda \delta_{1n}) \right)$$

$$\theta = \theta_c :$$

$$\frac{d u_n}{d \theta} = 2 \quad (96)$$

Equation (94) has been integrated explicitly for $n = 1, 2, 3, 4$.

While the integrations are somewhat laborious, there is no particular impediment to consideration of larger n . The results for the first four values of n are given below

$$u_1 = \theta_s G \left\{ -1 + \frac{\theta_s}{4\theta} + \frac{3}{4} \left(\frac{\theta^2 - \theta_b^2}{\theta_s^2 - \theta_b^2} \right)^{1/2} + \frac{2\theta^2 + \theta_b^2}{4\theta (\theta_s^2 - \theta_b^2)^{1/2}} \right. \\ \left. \cdot \ln \left(\frac{\theta_s + (\theta_s^2 - \theta_b^2)^{1/2}}{\theta + (\theta^2 - \theta_b^2)^{1/2}} \right) \right\} \quad (97a)$$

$$+ A_1 \theta^{-1} + B_1 \theta$$

$$u_2 = \theta_s G \theta^{-2} \left\{ \theta^2 - \frac{\theta^4}{2\theta_s^2} - \frac{\theta^4 (\theta_s^2 - \theta_b^2)}{2\theta_s^2 \theta_b^2} + \frac{2 (\theta^2 - \theta_b^2)^{5/2}}{5\theta_c^2 (\theta_s^2 - \theta_b^2)^{1/2}} \right. \\ \left. + \frac{\theta^4}{2\theta_b^2} - \frac{2(3\theta^2 + 2\theta_b^2)}{15\theta_b^2} \frac{(\theta^2 - \theta_b^2)^{3/2}}{(\theta_s^2 - \theta_b^2)^{1/2}} \right. \\ \left. - \frac{\theta^2 + 2\theta_b^2}{6} \left(\frac{\theta^2 - \theta_b^2}{\theta_s^2 - \theta_b^2} \right)^{1/2} \right. \quad (97b)$$

$$- \frac{\theta^4}{2\theta_c (\theta_s^2 - \theta_b^2)^{1/2}} \left(\tan^{-1} \left(\frac{\theta_s^2 - \theta_b^2}{\theta_b^2} \right) \right)^{1/2} \\ - \tan^{-1} \left(\frac{\theta^2 - \theta_b^2}{\theta_b^2} \right)^{1/2} \left. \right\} \frac{\theta_s}{\theta} + A_2 \theta^{-2} + B_2 \theta^2$$

$$\begin{aligned}
u_3 = \theta_s G \theta^{-3} \{ & \theta^3 - \frac{\theta^6}{2\theta_s \theta_b^2} + \frac{3\theta}{2\theta_b^2} \left(\frac{\theta^2 - \theta_b^2}{\theta_s^2 - \theta_b^2} \right)^{1/2} \left(\frac{\theta^2 - \theta_b^2}{3} \right)^2 \\
& + \frac{\theta_c^2 (\theta^2 - \theta_b^2)}{12} - \frac{\theta_b^4}{8} \} + \frac{3}{16} \frac{\theta_b^4}{(\theta_s^2 - \theta_b^2)^{1/2}} \\
& \cdot \ln \left(\frac{\theta_s + (\theta_s^2 - \theta_b^2)^{1/2}}{\theta + (\theta^2 - \theta_b^2)^{1/2}} \right) \frac{\theta_s}{\theta} \quad (97c) \\
& + A_3 \theta^{-3} + B_3 \theta^3
\end{aligned}$$

$$\begin{aligned}
u_4 = \theta_s G \theta^{-4} \{ & \theta^4 - \frac{4(3\theta^2 + 2\theta_b^2)}{15} \left(\frac{\theta^2 - \theta_b^2}{\theta_s^2 - \theta_b^2} \right)^{3/2} - \frac{\theta^8}{4\theta_b^2 \theta_s^2} \\
& - \frac{\theta^8}{4\theta_b^3 (\theta_s^2 - \theta_b^2)^{1/2}} \tan^{-1} \left(\frac{\theta^2 - \theta_b^2}{\theta_b^2} \right)^{1/2} \quad (97d) \\
& + \frac{2(\theta^2 - \theta_b^2)^{3/2}}{(\theta_s^2 - \theta_b^2)^{1/2}} \left(\frac{\theta^2 - \theta_b^2}{7\theta_b^2} \right)^2 + \frac{2(\theta^2 - \theta_b^2)}{5} \\
& + \frac{\theta_b^2}{3} \} - \frac{1}{4\theta_b^2} \left(\frac{\theta^2 - \theta_b^2}{\theta_s^2 - \theta_b^2} \right)^{1/2} \left(\frac{\theta^2 - \theta_b^2}{7} \right)^3 \\
& + \frac{3\theta_b^2 (\theta^2 - \theta_b^2)^2}{5} + \theta^2 \theta_b^4 \} \frac{\theta_s}{\theta} \\
& + A_4 \theta^{-4} + B_4 \theta^4
\end{aligned}$$

The constants of integration A_n and B_n are given by

$$A_n = \frac{\theta_s^n}{2} \left(u_n - \frac{\theta}{n} \frac{du_n}{d\theta} \right)_{\theta=\theta_s} \quad (98)$$

$$B_n = \frac{\theta_s^{-n}}{2} \left(u_n + \frac{\theta}{n} \frac{du_n}{d\theta} \right)_{\theta=\theta_s} \quad (99)$$

Having determined the u_n , we can compute v_n , w_n , a_n , C_{p_n} , and $\theta_{n_b}/\theta_{n_s}$ from Eqs. (66), (62), (58), (69), and (96), respectively.

We are particularly interested in the shock shape - body shape relation ($\theta_{n_b}/\theta_{n_s}$), surface pressure coefficient (C_{p_n}), and flow streamsurfaces. The first two quantities can be easily measured while the latter quantity is useful in developing waverider geometries.

Differentiating Eqs. (97) with respect to θ , we obtain expression for v_1 , v_2 , v_3 , and v_4 . Evaluating these expressions at $\theta = \theta_c$, we can determine the ratio of the body perturbation to the shock perturbation, $\theta_{n_c}/\theta_{n_s}$. The results are

$$\begin{aligned} \frac{\theta_{1b}}{\theta_{1s}} = 1 + (1-\lambda) \left\{ G \left[-\frac{n^2}{8} + \frac{n}{8(n^2-1)^{1/2}} \ln(n + (n-1)^{1/2}) \right] \right. \\ \left. + \frac{n^2-1}{4} + \frac{n^4-1}{4n^2} \frac{2-(\gamma-1)K_s^2}{2+(\gamma-1)K_s^2} \right\} \end{aligned} \quad (99a)$$

$$\begin{aligned} \frac{\theta_{2b}}{\theta_{2s}} = G \left[-\frac{n(n^2+2)}{6} + \frac{n}{2(n^2-1)^{1/2}} \tan^{-1}((n^2-1)^{1/2}) \right] \\ + \frac{n^4-1}{2n^3} + \frac{n^4+1}{4n} \left(\frac{n^2+1}{n^2} + \frac{n^2-1}{n^2} \frac{2-(\gamma-1)K_s^2}{2+(\gamma-1)K_s^2} \right) \end{aligned} \quad (99b)$$

$$\frac{\theta_{3b}}{\theta_{3s}} = G \left[\frac{3}{4} - \frac{3}{16} \eta^4 - \frac{9}{32} \eta^2 - \frac{9}{32} \frac{\eta}{(\eta^2-1)^{1/2}} \ln(\eta+(\eta^2-1)^{1/2}) \right] \quad (99c)$$

$$+ \frac{3}{4} \frac{\eta^6-1}{\eta^4} + \frac{\eta^6+1}{4 \eta^2} \left(\frac{\eta^2+1}{\eta^2} + \frac{\eta^2-1}{\eta^2} \frac{2-(\gamma-1) K_s^2}{2+(\gamma-1) K_s^2} \right)$$

$$\frac{\theta_{4b}}{\theta_{4s}} = G \left[\frac{1}{2\eta} + \frac{\eta^3}{2} - 2 \eta^5 + \frac{\eta^7}{2} + 8 (\eta^2-1) \left(\frac{13\eta^3}{80} - \frac{\eta^5}{16} + \frac{23\eta}{15} \right) \right. \quad (99d)$$

$$\left. + \frac{\eta}{2(\eta^2-1)^{1/2}} \tan^{-1} \left((\eta^2-1)^{1/2} \right) \right] + \frac{\eta^8-1}{\eta^5}$$

$$+ \frac{\eta^8+1}{4 \eta^3} \left(\frac{\eta^2+1}{\eta^2} + \frac{\eta^2-1}{\eta^2} \frac{2-(\gamma-1) K_s^2}{2+(\gamma-1) K_s^2} \right)$$

where η is the ratio of the shock angle to the cone angle for the unperturbed right circular cone,

$$\eta = \frac{\theta_s}{\theta_b} \quad (100)$$

and is given by Eq. (91) as a function of K_b . Typical results obtained from Eqs. (99) are shown in Figure 4 for $\gamma = 1.4$. Note that the linearized theory result $\theta_{n_s}/\theta_{n_b} = 0$ is obtained for $K_b = 0$. Also as η increases, the relative distortion of the shock shape decreases. Other numerical results, not shown here, show that these results are not very sensitive to changes in γ for γ in the range of $9/7$ to $5/3$.

Equations (67) - (69) can be used to evaluate the surface pressure coefficient. Rewriting these results in the hypersonic small disturbance theory similarity form,

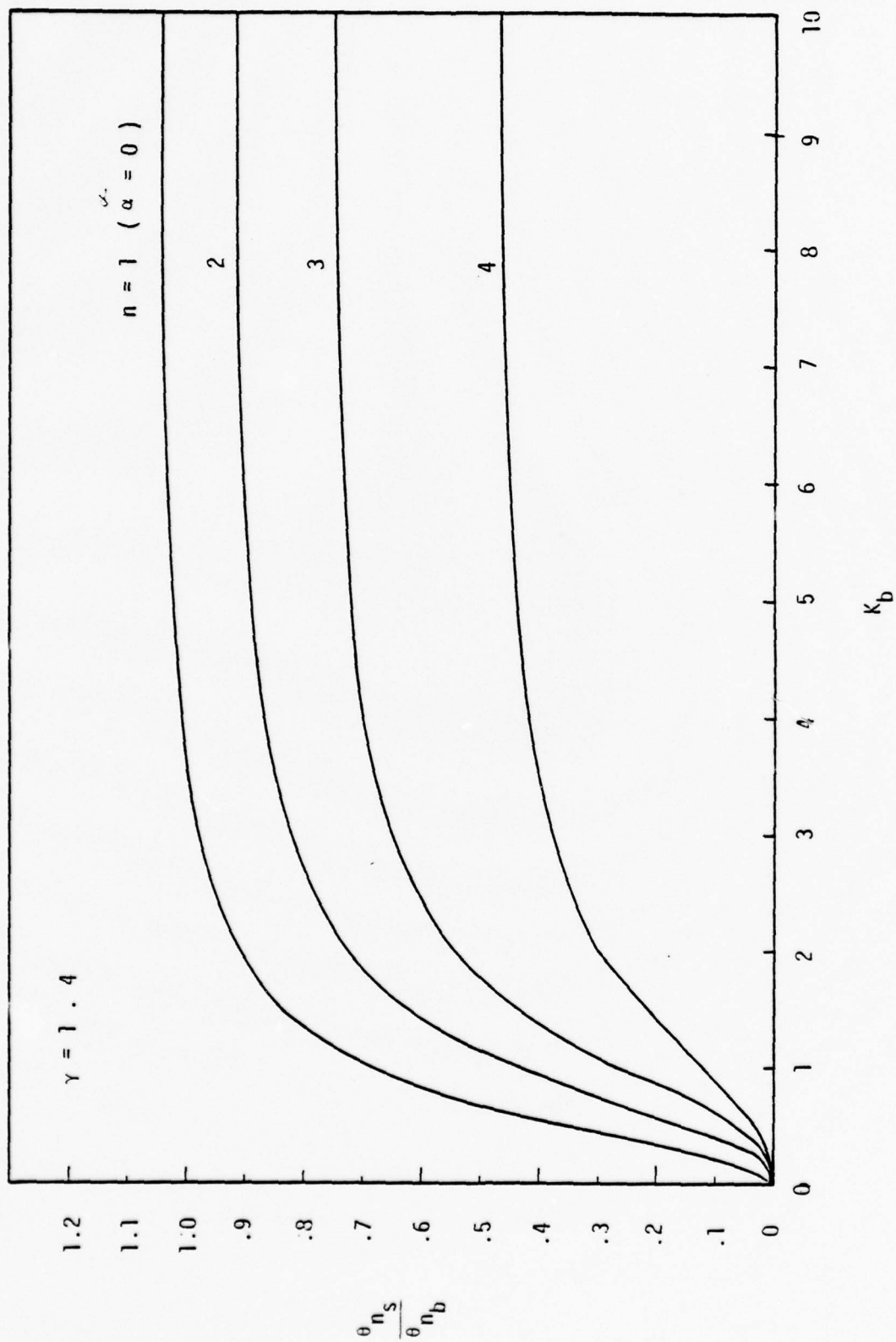


FIGURE 4. RELATION BETWEEN SHOCK AND BODY SHAPES ($K_b = M_1 \theta_{o_b}$)

$$\frac{C_p}{\theta_b^2} = \frac{C_{p0}}{\theta_b^2} + \sum_n \frac{C_{pn}}{\theta_b} \frac{\theta_{nb}}{\theta_b} \cos n \phi + \sum_m \frac{C_{pm}}{\theta_b} \frac{\theta_{mb}}{\theta_b} \sin m \phi \quad (101)$$

we have, on the surface of the body,

$$\frac{C_{p0}}{\theta_b^2} = 1 + \frac{(\gamma+1) K_b^2 + 2}{(\gamma-1) K_b^2 + 2} \ln \left(\frac{\gamma+1}{2} + \frac{1}{K_b^2} \right) \quad (102)$$

$$\begin{aligned} \frac{C_{pn}}{\theta_b} = -n \frac{\theta_{nb}}{\theta_{ns}} \left(\frac{C_{p0}}{\theta_b^2} + \frac{2}{\gamma K_b^2} \right) & \left[\frac{4\gamma(K_s^2-1)^2(1-\lambda \delta_{1n})}{(2\gamma K_s^2 - \gamma+1)((\gamma-1) K_s^2 + 2)} \right. \\ & \left. + \frac{u_n(\theta_b)}{\theta_s} \frac{\gamma K_s^2}{1 + \frac{\gamma-1}{2} K_b^2 (1 + \ln \frac{K_s^2}{K_b^2})} \right] \quad (103) \end{aligned}$$

where n and θ_{nb}/θ_{ns} are given as functions of K_b by Eqs. (91) and (99) respectively. The radial component u_n of the perturbation velocity is given on the body surface by

$$\begin{aligned} \frac{u_n(\theta_b)}{\theta_s} = (1-\lambda) \left\{ G \left[n-1 - \frac{3}{4} \left(n - \frac{1}{(n^2-1)^{1/2}} \ln(n+(n^2-1)^{1/2}) \right) \right] \right. \\ \left. - \frac{n^2+1}{2n} - \frac{(n^2-1)^2}{2n^3} \frac{2 - (\gamma-1) K_s^2}{2 + (\gamma-1) K_s^2} \right\}, n=1 \quad (104a) \end{aligned}$$

$$= G \left[n^2-1 + \frac{(n^2+1)(n^2-1)^2}{2n^2} - \frac{n^2(n^2-1)}{2} + \frac{(n^2-1)^2}{10} \right]$$

$$- \frac{(n^2-1)(3n^2+2)}{30} + \frac{(n^2-1)}{2n^2} - \frac{n^2+2}{6} \quad (104b)$$

$$+ \frac{1}{2(n^2-1)^{1/2}} \tan^{-1} ((n^2-1)^{1/2})]$$

$$- \frac{n^4+1}{2n^2} - \frac{n^4-1}{4n^4} (n^2+1 + (n^2-1) \frac{2-(\gamma-1) K_s^2}{2+(\gamma-1) K_s^2})$$

, n=2

$$= G [n^3 - 1 - \frac{n^6-1}{2n} + \frac{n}{2} (n^2-1) (n^2 - \frac{3}{4}) \quad (104c)$$

$$- \frac{3}{16} (n - \frac{1}{(n^2-1)^{1/2}} \ln (n + (n^2-1)^{1/2}))]$$

$$- \frac{n^6+1}{2n^5} - \frac{n^6-1}{6n^5} (n^2+1 + (n^2-1) \frac{2-(\gamma-1) K_s^2}{2+(\gamma-1) K_s^2}) , n = 3$$

$$= G [n^4 - 1 - \frac{4}{15} (n^2-1)(3n^2+2) - \frac{n^8-1}{4n^2} - \frac{(n^2-1)^2}{4} \quad (104d)$$

$$\cdot (\frac{n^2-1}{7} + \frac{3}{5}) + 2 (n^2-1) (\frac{(n^2-1)^2}{7} + \frac{2(n^2-1)}{5} + \frac{1}{3})$$

$$- \frac{1}{4} (n^2 - \frac{1}{(n^2-1)^{1/2}} \tan^{-1} ((n^2-1)^{1/2}))] - \frac{n^8+1}{2n^6}$$

$$- \frac{n^8-1}{8n^6} (n^2+1 - (n^2-1) \frac{2-(\gamma-1) K_s^2}{2+(\gamma-1) K_s^2}) , n = 4$$

Typical results for the surface pressure coefficient are shown in Figure 5 for $\gamma = 1.4$. These results achieve a hypersonic limiting value as $K_b \rightarrow \infty$ which agrees well with other known solutions. For example, for $n = 1$, our result C_{p1} / θ_{ob} takes on the value 4.046 which is to be compared with 4.088 obtained by Cheng (8) in a separate analysis. The linearized limit, $K_b \rightarrow 0$, of Eq. (103) yields

$$\frac{C_{pn}}{b} \rightarrow \frac{4}{n} \text{ as } K_b \rightarrow 0 \quad (105)$$

This result agrees exactly with the linearized theory result of Mascitti (9).

Figure 6 shows a comparison of the present theory with the experimental results obtained by Chan (10) for flow past a right circular cone of half angle $\theta_b = 15^\circ$ and freestream Mach number $M_1 = 10.4$ and various angles of attack. Provided the angle of attack is small compared to θ_{ob} , this flow corresponds to a shock wave whose shape deviates from a circle (in cross-section) by an amount proportional to $\cos \phi$. Figure 6 compares results from the present theory for the surface pressure coefficient for $n = 1$ with experimental results for $\alpha / \theta_{ob} = 0, 0.2, 0.4$. The comparison is quite good, although the error does grow as α / θ_{ob} increases, particularly near the symmetry lines ($\theta = 0, \pi$).

Figures 7 - 10 compare the present theory for $n = 2$ with experiments (11) and a purely numerical solution (12) for flow past an elliptic cone. Provided the eccentricity e of the elliptic cone is small, the cone shape can be approximated by a Fourier expansion

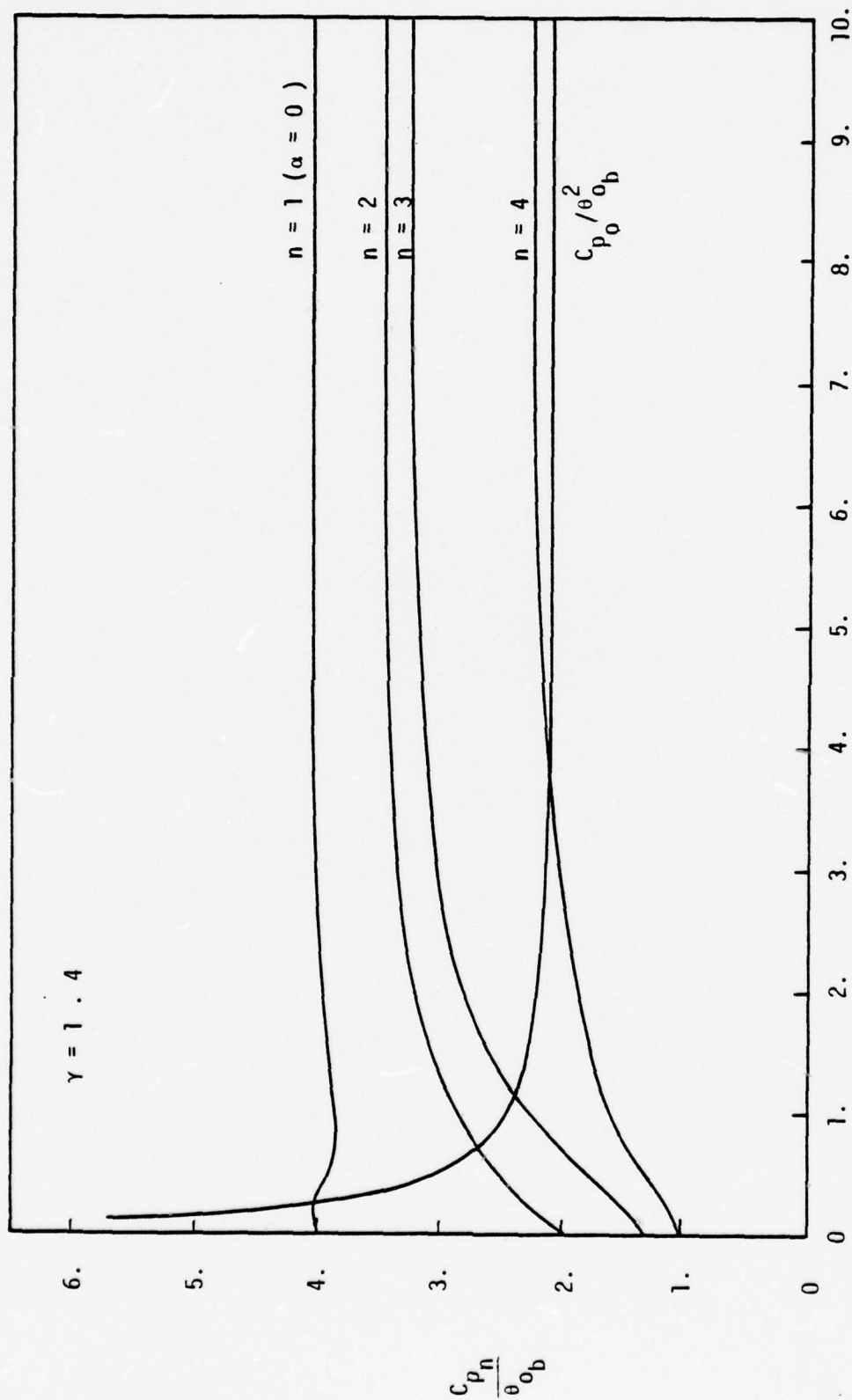


FIGURE 5. SURFACE PRESSURE COEFFICIENT ($K_b = M_1 \theta_{o_b}$)

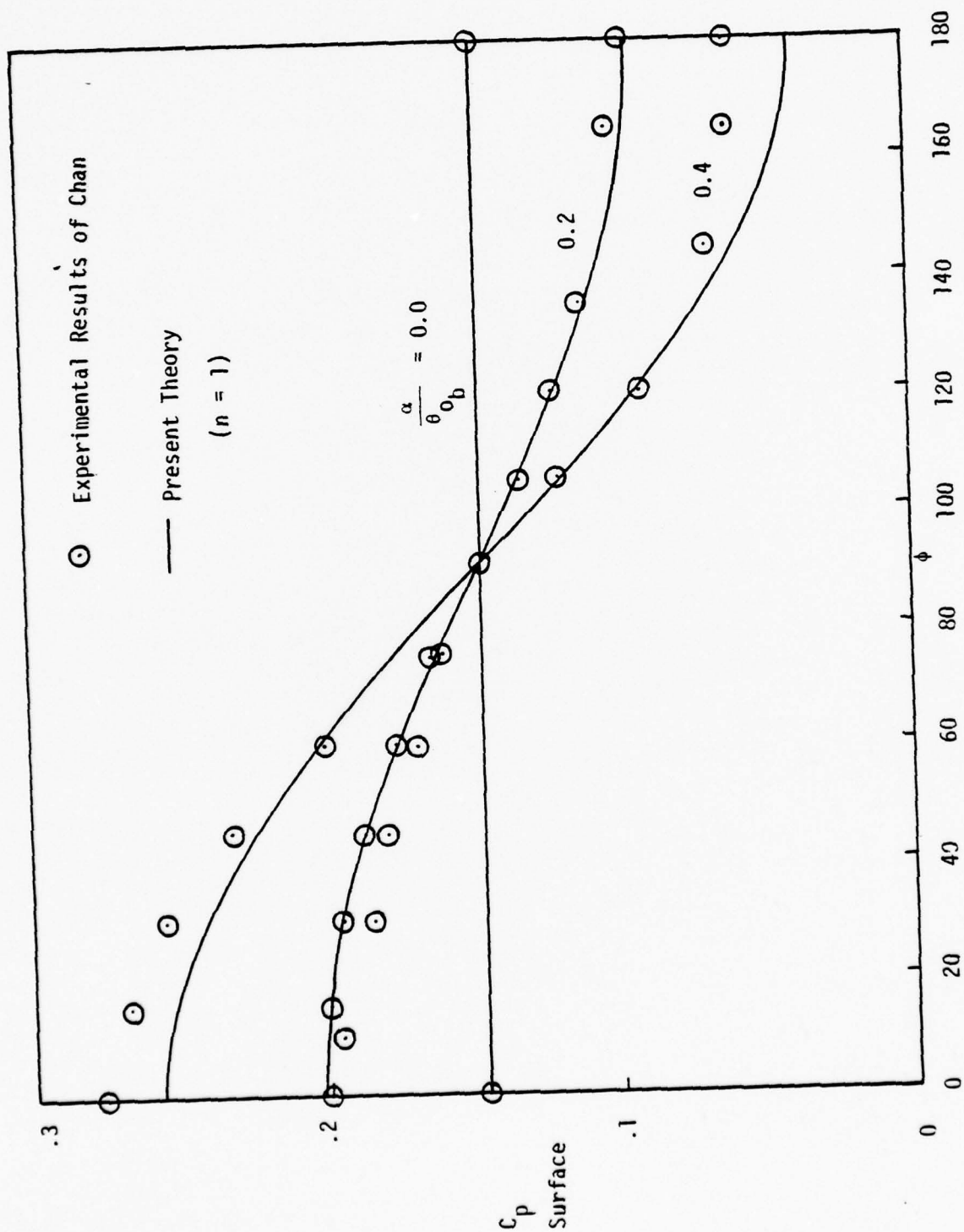


FIGURE 6. CIRCULAR CONE AT ANGLE OF ATTACK. COMPARISON OF THEORY AND EXPERIMENT

$$\theta_b(\phi) = \theta_{0b} + \theta_{2b} \cos 2\phi + \theta_{4b} \cos 4\phi + \dots \quad (106)$$

where (see Lee and Rasmussen (4)),

$$\theta_{0b} = \theta_m + \frac{e^2}{32} (3 - 2 \sin^2 \theta_m) \sin 2\theta_m + \mathcal{O}(e^4) \quad (107)$$

$$\theta_{2b} = \frac{e}{4} \left[1 + \frac{e^2}{32} (15 - 20 \sin^2 \theta_m + 8 \sin^4 \theta_m) + \mathcal{O}(e^4) \right] \sin 2\theta_m$$

$$\theta_{4b} = \frac{e^2}{32} \left[(3 - 2 \sin^2 \theta_m) + \mathcal{O}(e^2) \right] \sin 2\theta_m$$

Here

$$\theta_m = \tan^{-1} \frac{\sqrt{2ab}}{(a^2 + b^2)^{1/2}} \quad (108)$$

$$e = \frac{b^2 - a^2}{b^2 + a^2}$$

and $a \equiv \tan \theta_a$ and $b \equiv \tan \theta_b$ are the semiminor and semimajor axes. Provided e is small, the elliptic cone can be represented by the first two terms of the expansion. The third Fourier coefficient, θ_{4b} , is of order e^2 and thus is neglected in our perturbation analysis. The experiments of Zakkay and Visich (11) used two different elliptic ones, each cone being run at two Mach numbers. Thus four comparisons are possible as shown in Table 1 below.

TABLE 1: Experimental Conditions in Zakkay and Visich (11).

Model Mach Number	$a = .2555$ $b = .3562$ $\theta_{0b} = .2911$ $\theta_{2b} = .0453$ $\theta_{4b} = .0091$	$a = .2256$ $b = .4034$ $\theta_{0b} = .2873$ $\theta_{2b} = .0758$ $\theta_{4b} = .0245$
3.09	Case 1	Case 2
6.00	Case 3	Case 4

The results shown in Figures 7 - 10 show that the comparison between experiment and the present theory is reasonable, although not perfect. The trends clearly are depicted correctly. The largest differences between theory and experiment occur near $\phi = 45^\circ$. This suggests that second-order terms (e.g. terms of order θ_{2b}^2 and θ_{4b}) may be important as they give rise to $\cos 4\phi$ contributions which are a maximum at $\phi = 45^\circ$. The present theory does not allow us to estimate the contribution of terms of order θ_{2b}^2 , although the contribution of the θ_{4b} term can be computed. If we compare θ_{2b}^2 and θ_{4b} for the two

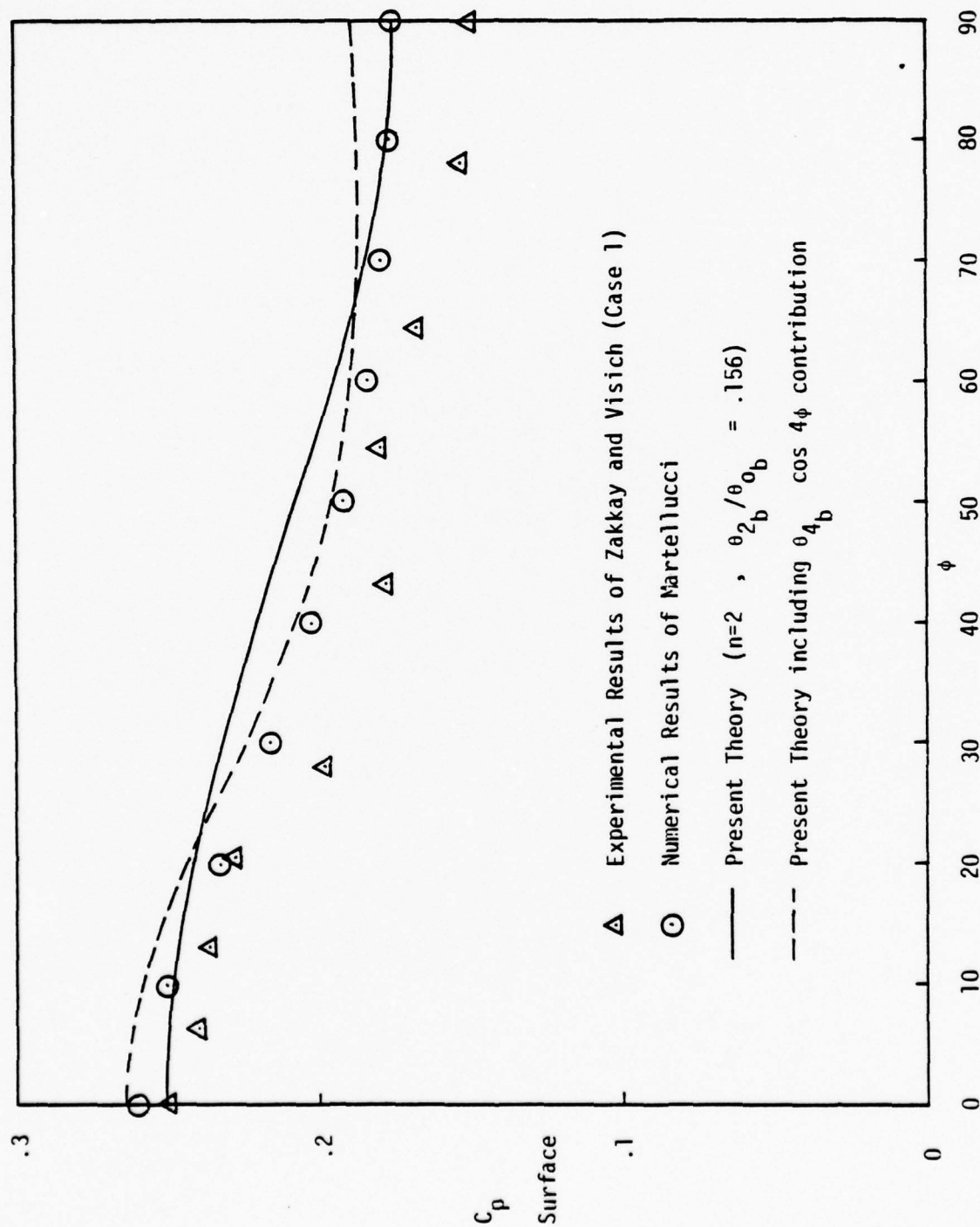


FIGURE 7. ELLIPTICAL CONE. COMPARISON OF THEORY AND EXPERIMENT (Case 1, Ref. 11)

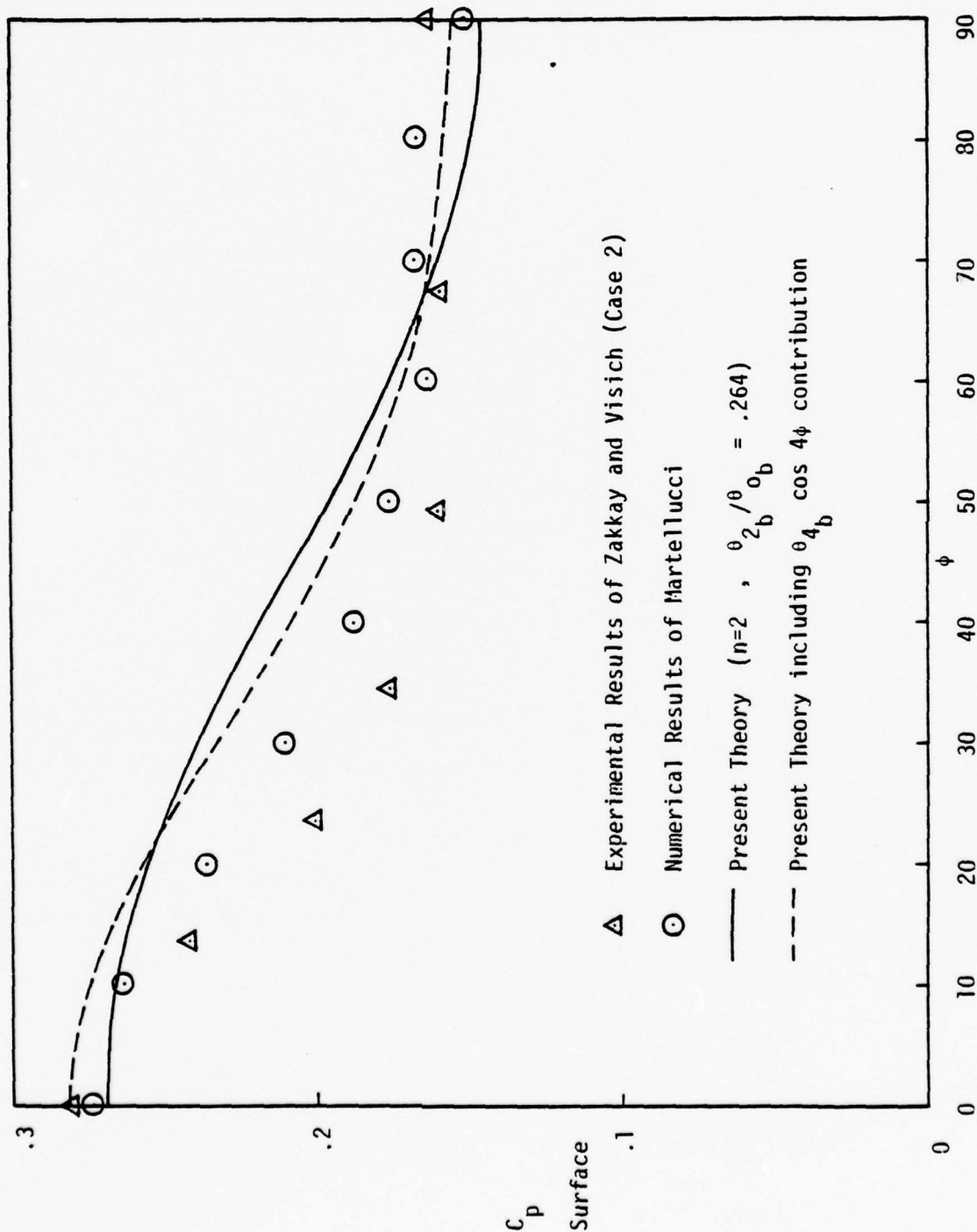


FIGURE 3. ELLIPTICAL CONE. COMPARISON OF THEORY AND EXPERIMENT (Case 2. Ref. 11)

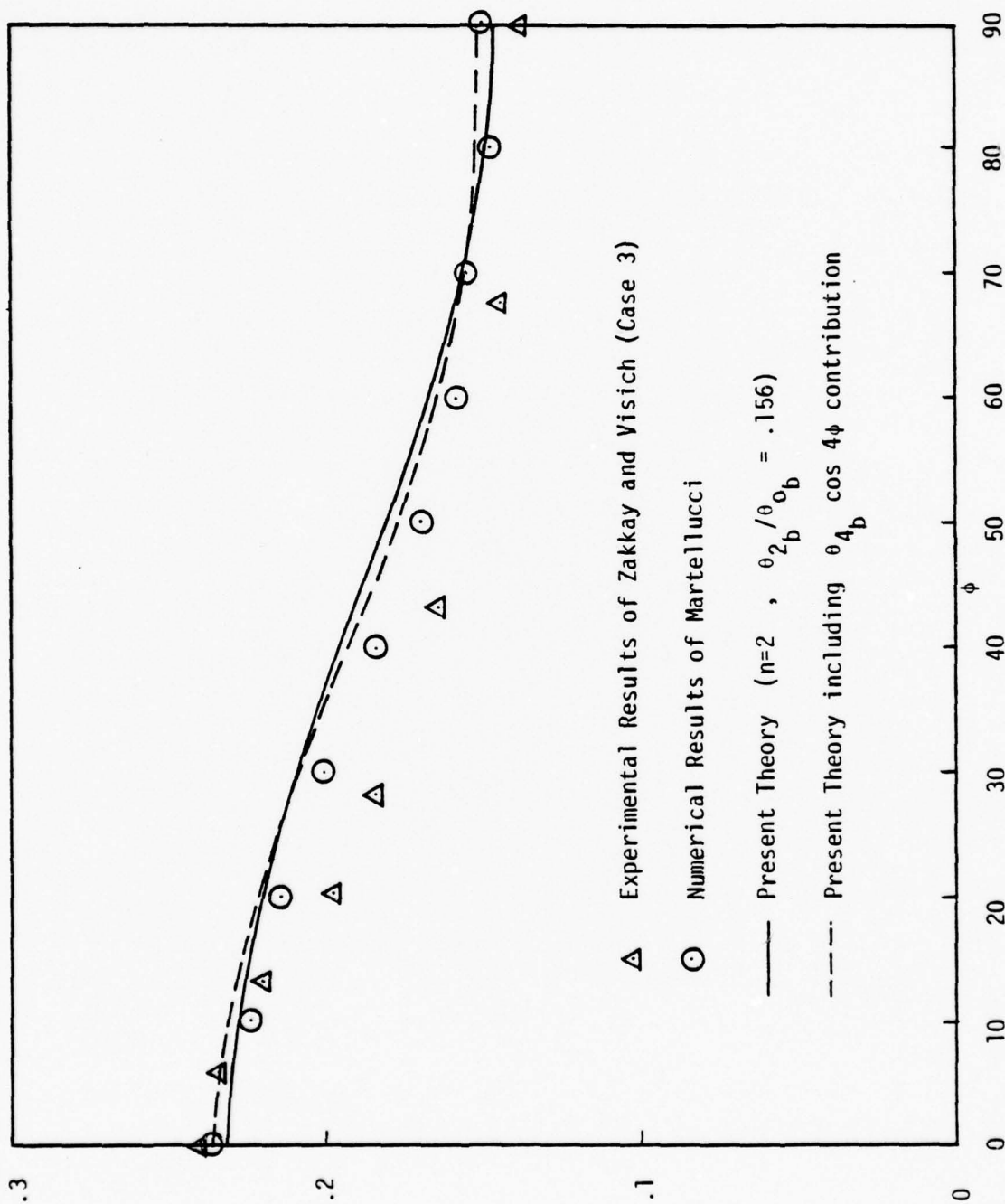


FIGURE 9. ELLIPTICAL CONE. COMPARISON OF THEORY AND EXPERIMENT (Case 3, Ref. 11)

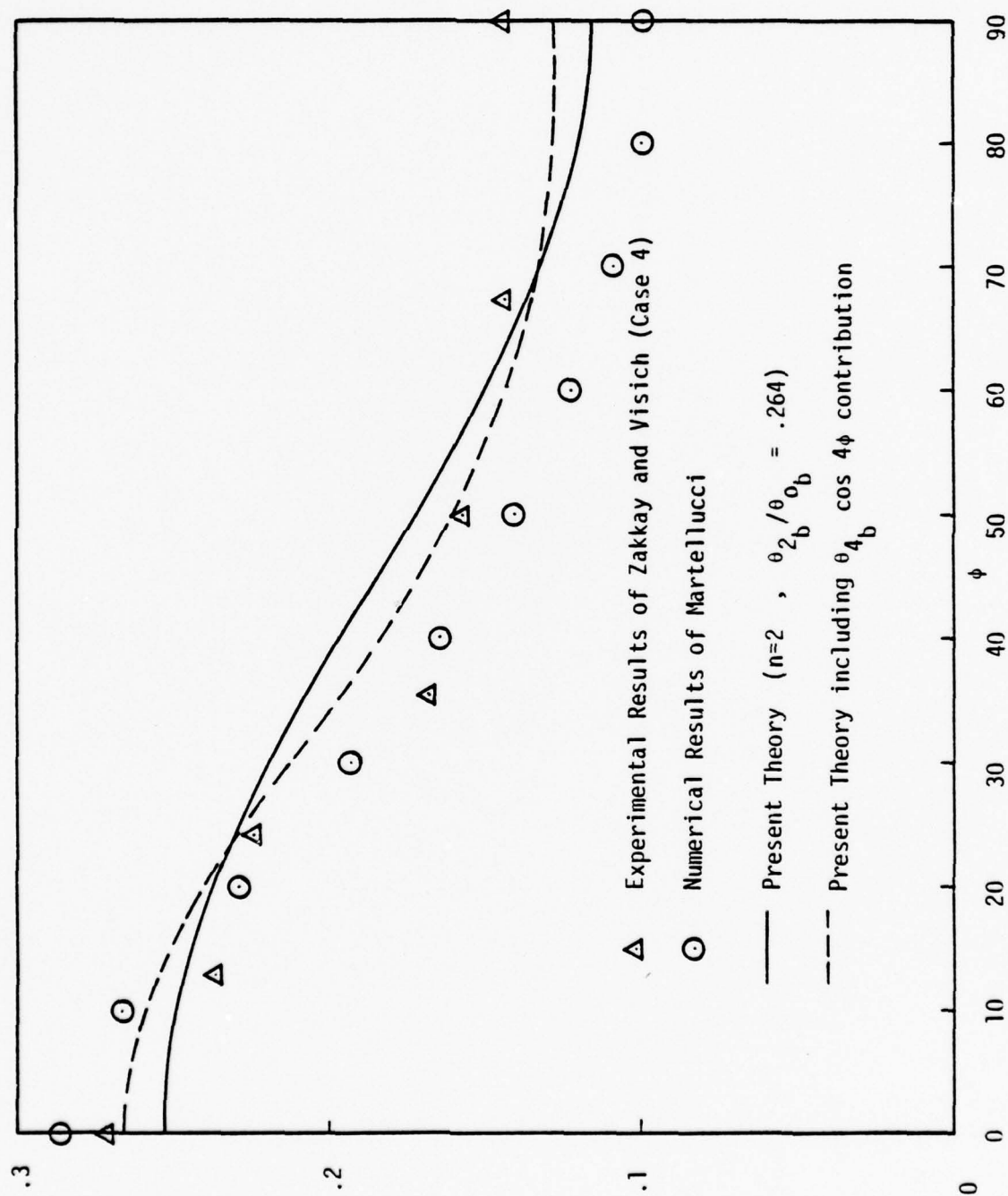


FIGURE 10. ELLIPTICAL CONE. COMPARISON OF THEORY AND EXPERIMENT (Case 4, Ref. 11)

models used by Zakkay and Visich, we see that θ_{2b}^2 equals $0.23 \theta_{4b}$. This suggests that the θ_{4b} contribution is the most important of the two second-order corrections.

Figures 7 - 10 show the effect of including the $\theta_{4b} \cos 4 \phi$ contribution. That is, the dashed lines in Figures 7 - 10 give $(C_{p_0} + C_{p_2} \theta_{2b} \cos 2 \phi + C_{p_4} \theta_{4b} \cos 4 \phi)$. In general, inclusion of the $\theta_{4b} \cos 4 \phi$ term improves the agreement between theory and experiment, especially on the windward generators. However, disagreement between theory and experiment remains near $\phi = 45^\circ$. The causes of this disagreement are not clear although viscous effects, model misalignment, and nonuniform test conditions are possible explanations in addition to the second-order terms ignored in the present analysis.

SECTION 6

STREAMSURFACES AND WAVERIDER GEOMETRIES

The streamsurfaces of the flowfield are surfaces composed of streamlines which, in turn, are the field lines of the velocity vector. The streamlines of a given velocity field can be determined from the solution of

$$\vec{dr} \times \vec{V} = 0 \quad (109)$$

where \vec{r} is a vector giving position along the streamline. In spherical polar coordinates Eq. (109) can be reduced to

$$\frac{dr}{u} = \frac{r d\theta}{v} = \frac{r \sin \theta d\phi}{w} \quad (110)$$

It is convenient in the present analysis to introduce a new polar coordinate $\bar{\theta}$, defined as

$$\bar{\theta} = \frac{\theta - \theta_b(\phi)}{\theta_s(\phi) - \theta_b(\phi)} \quad (111)$$

Then $\bar{\theta}$ varies from zero on the body to unity at the shock. Now

$$d\theta = (\theta_s - \theta_b) \left[d\bar{\theta} + \left(\frac{\theta'_b}{\theta_b - \theta_s} + \bar{\theta} \frac{\theta'_s - \theta'_b}{\theta_s - \theta_b} \right) d\phi \right] \quad (112)$$

For geometries which deviate slightly from that of a right circular cone, $\theta_b = \theta_{0b} + \mathcal{V}(\theta_{nb}, \theta_{mb})$ and $\theta_s = \theta_{0s} + \mathcal{V}(\theta_{ns}, \theta_{ms})$. In this case, Eq. (112) reduces to

$$d\theta = (\theta_{o_s} - \theta_{o_b}) d\bar{\theta} + \mathcal{V}(\theta_{n_b}, \theta_{m_b}). \quad (113)$$

and Eq. (110) becomes

$$\frac{dr}{u} = \frac{r(\theta_{o_s} - \theta_{o_b})}{v} d\bar{\theta} = \frac{r \sin((\theta_{o_s} - \theta_{o_b}) \bar{\theta})}{w} d\phi \quad (114)$$

with errors of order $(\theta_{n_b}, \theta_{m_b})$. The velocity field is given by Eqs. (46),

$$\begin{aligned} u &= u_0 + \sum_{\theta_{n_b}} u_n \cos n\phi + \sum_{\theta_{m_b}} u_m \sin m\phi \\ v &= v_0 + \sum_{\theta_{n_b}} v_n \cos n\phi + \sum_{\theta_{m_b}} v_m \sin m\phi \\ w &= \sum_{\theta_{n_b}} w_n n \sin n\phi - \sum_{\theta_{m_b}} w_m m \cos m\phi \end{aligned} \quad (115)$$

Thus, to lowest order, Eqs. (114) becomes

$$\frac{dr}{r} = (\theta_{o_s} - \theta_{o_b}) \frac{u_0}{v_0} d\bar{\theta} + \mathcal{V}(\theta_{n_b}, \theta_{m_b}) \quad (116)$$

$$\begin{aligned} \frac{(\theta_{o_s} - \theta_{o_b}) d\bar{\theta}}{v_0 \sin((\theta_{o_s} - \theta_{o_b}) \bar{\theta})} &= \frac{d\phi}{\sum_{\theta_{n_b}} w_n n \sin n\phi - \sum_{\theta_{m_b}} w_m m \cos m\phi} \\ &\quad + \mathcal{V}(\theta_{n_b}, \theta_{m_b}) \end{aligned} \quad (117)$$

Equation (116) can be integrated to give

$$r = r_i \exp\left((\theta_{o_s} - \theta_{o_b}) \int_{\bar{\theta}_i}^{\bar{\theta}} \frac{u_0}{v_0} d\bar{\theta}\right) \quad (118)$$

where r_i and $\bar{\theta}_i$ are constants of integration and correspond to the streamline passing through the point $(r_i, \bar{\theta}_i, \phi_i)$. Integration of Eq. (117) is impossible, in general. However, for geometries that can be represented by a single Fourier component in ϕ , a rather simple result can be obtained,

$$\tan\left(\frac{n\phi}{2}\right) = \tan\left(\frac{n\phi_i}{2}\right) \exp \left[\theta_{nb} n^2 (\theta_{os} - \theta_{ob}) \int_{\bar{\theta}_i}^{\bar{\theta}} \frac{w_n d\bar{\theta}}{v_o \sin\left(\frac{(\theta_{os} - \theta_{ob})}{\theta} \bar{\theta}\right)} \right] \quad (119)$$

Using the hypersonic small disturbance theory approximation, the integrals that appear in Eqs. (118) and (119) can be evaluated approximately.

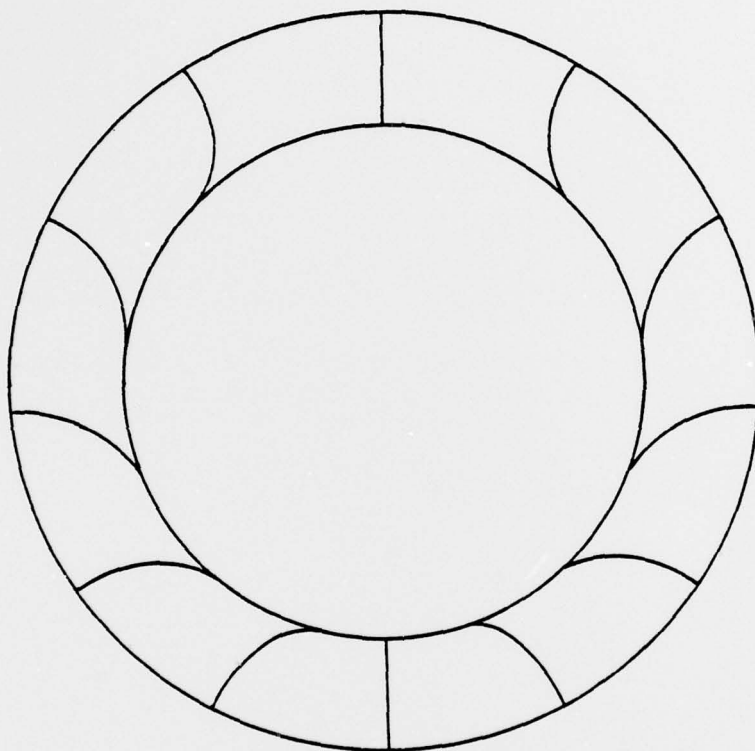
There results

$$\frac{r}{r_i} = \left(\frac{\theta_i^2 - \theta_b^2}{\theta^2 - \theta_b^2} \right)^{\frac{1}{2}} \quad (120)$$

$$\tan\left(\frac{n\phi}{2}\right) = \tan\left(\frac{n\phi_i}{2}\right) \left(\frac{\theta_i^2 - \theta_b^2}{\theta^2 - \theta_b^2} \right)^{\frac{n^2 \theta_{nb} (F_o - u_n)_b}{2 \theta_{ob}^2}} \quad (121)$$

Here we have rewritten the results in terms of θ rather than $\bar{\theta}$. Also, in carrying out the integration in Eq. (119), we have approximated $(F_o - u_n)$ by its value on the body.

Typical results from Eq. (121) are shown in Figure 11-14 for $n = 1, 2, 3, 4$, respectively. These results give the projection of the streamlines on the unit sphere. We refer to these projections as the "crossflow streamlines". For a given n , the number of crossflow stagnation points is $2n$. One-half of the stagnation points are of the saddle point variety while the other half are of the improper node type.



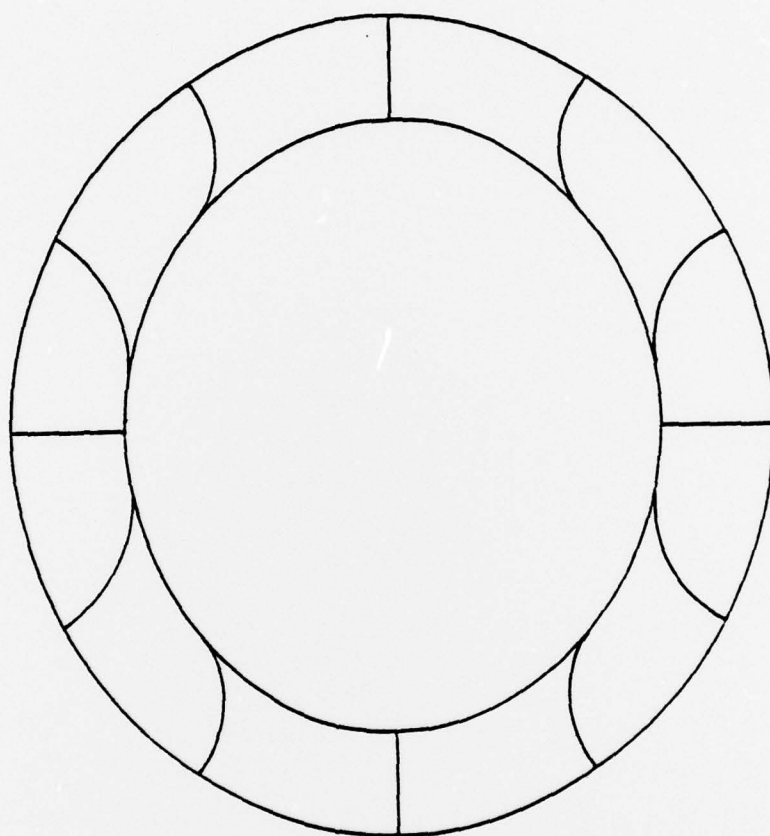
$$M_1 \theta_{ob} = 1.0$$

$$\theta_{ob} = 15^\circ$$

$$\theta_{1b} = 1.5^\circ$$

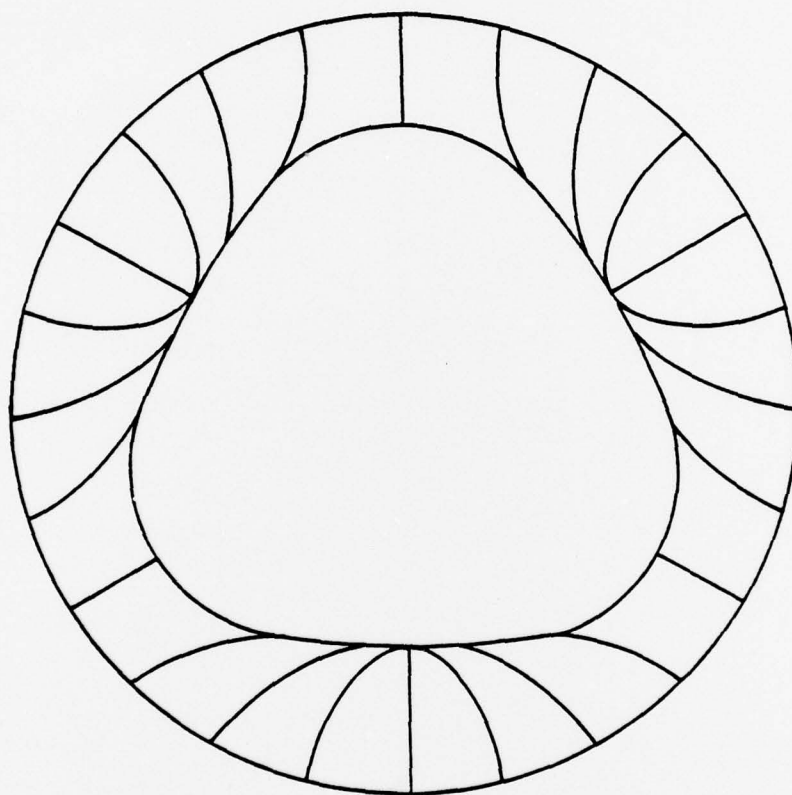
$$\gamma = 1.4$$

FIGURE 11. CROSSFLOW STREAMLINES, $\theta_b = \theta_{ob} + \theta_{1b} \cos \phi$.



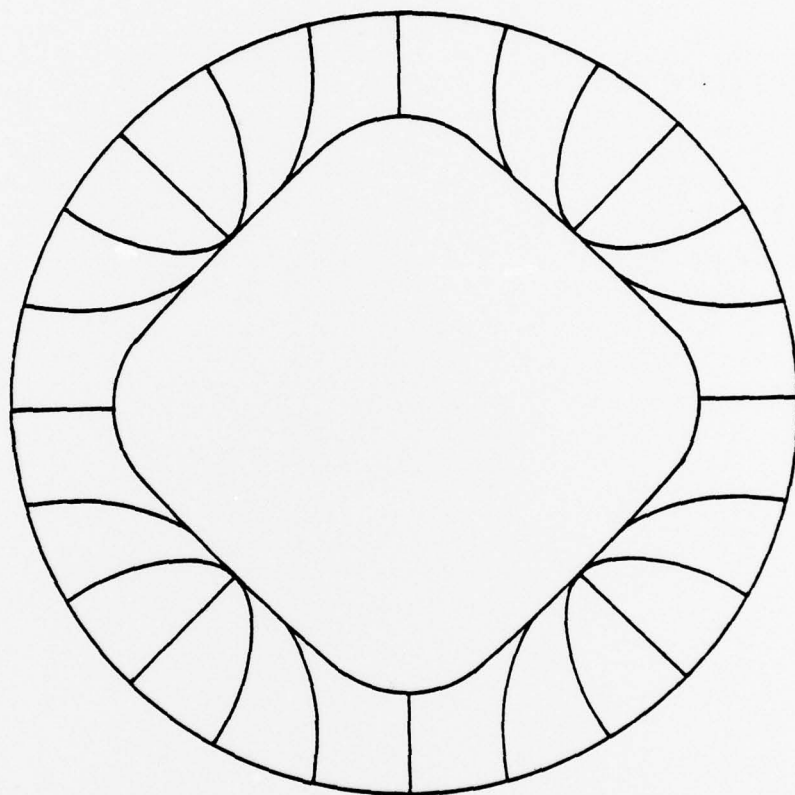
$$\begin{aligned}
 M_1 \theta_{0b} &= 1.0 \\
 \theta_{0b} &= 15^\circ \\
 \theta_{2b} &= 1.5^\circ \\
 \gamma &= 1.4
 \end{aligned}$$

FIGURE 12. CROSSFLOW STREAMLINES, $\theta_b = \theta_{0b} + \theta_{2b} \cos 2\phi$.



$$\begin{aligned}
 M_1 \theta_{0b} &= 1.0 \\
 \theta_{0b} &= 15^\circ \\
 \theta_{3b} &= 1.5^\circ \\
 \gamma &= 1.4
 \end{aligned}$$

FIGURE 13. CROSSFLOW STREAMLINES, $\theta_b = \theta_{0b} + \theta_{3b} \cos 3\phi$.



$$\begin{aligned}
 M_1 \theta_{ob} &= 1.0 \\
 \theta_{ob} &= 15^\circ \\
 \theta_{4b} &= 1.5^\circ \\
 \gamma &= 1.4
 \end{aligned}$$

FIGURE 14. CROSSFLOW STREAMLINES, $\theta_b = \theta_{ob} + \theta_{4b} \cos 4\phi$.

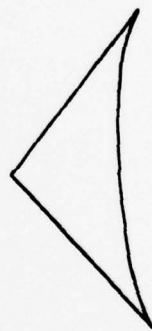
These crossflow streamline results can be used to develop a series of new waverider geometries. That is, since the streamlines of any inviscid flow can be interpreted as a solid boundary, we can use these streamlines to generate new lifting body shapes. While the generation of the new lifting body shapes will be the subject of a subsequent report, Figure 15 shows sketches of some possible results.



$$(a). \quad \theta_b = \theta_{0b} + \theta_{1b} \cos \phi$$



$$(b) \quad \theta_b = \theta_{0b} + \theta_{2b} \cos 2\phi$$



$$(c) \quad \theta_b = \theta_{0b} + \theta_{3b} \cos 3\phi$$



$$(d) \quad \theta_b = \theta_{0b} + \theta_{4b} \cos 4\phi$$

FIGURE 15. WAVERIDER GEOMETRIES DERIVED FROM FLOWS PAST CONICAL BODIES THAT DEVIATE SLIGHTLY FROM A RIGHT CIRCULAR CONE (freehand sketches)

SECTION 7

CONCLUDING REMARKS

The results obtained should be particularly useful because of their simplicity and ease of utility. The determination of the forces acting on a body has been reduced to rather simple formulas. The dependence of the pressure force on the body shape, free-stream conditions, and ratio of specific heats is explicitly demonstrated. In addition, the associated streamsurfaces allow new classes of lifting bodies to be developed by means of the waverider notion. In this way, practical lifting geometries can be developed which avoid shape corners, wings of zero thickness, and other unrealistic features.

Comparison of these new geometries and waveriders with experiment remains to be accomplished. The necessary experiments are not particularly difficult or unusual. However, they are essential both to verify the theoretical calculations and well as to determine whether these waveriders give stable, lifting flow at off-design conditions.

ACKNOWLEDGEMENTS

The author wishes to acknowledge many beneficial discussions with his colleague, Maurice L. Rasmussen.

REFERENCES

1. Ferri, A., Ness, N., and Kaptita, T., "Supersonic Flow Over Conical Bodies without Axial Symmetry". Journal of the Aeronautical Sciences, Vol. 20, No. 8, Aug. 1953, pp 563-571.
2. Chapkis, R.T., "Hypersonic Flow Over an Elliptic Cone: Theory and Experiment". Journal of the Aeronautical Sciences, Vol. 28, No. 11, Nov. 1961, pp. 844-854.
3. Doty, R. T. and Rasmussen, M.L., "Approximation for Hypersonic Flow Past an Inclined Cone", Journal of the American Institute of Aeronautics and Astronautics, Vol. 11, No. 9, Sept. 1973, pp. 1310-1315. (AIAA Journal)
4. Lee, H.M. and Rasmussen, M.L., "Hypersonic Flow Past an Elliptic Cone", AIAA Paper 79-0364, January, 1979.
5. Munson, A.G., "The Vortical Layer on an Inclined Cone", Journal of Fluid Mechanics, Vol. 20, 1964, pp. 625 - 643.
6. Melnik, R.E., "Vortical Singularities in Conical Flow", AIAA Journal, Vol. 5, No. 4, April 1967, pp. 631-637.
7. Rasmussen, M.L., "On Hypersonic Flow Past an Unyawed Cone", AIAA Journal, Vol. 5, No. 8, Aug. 1967, pp. 1495-1497.
8. Cheng, H.K., "Hypersonic Flows Past a Yawed Circular Cone and Other Pointed Bodies", Journal of Fluid Mechanics, Vol. 12, 1962, pp. 169-191.
9. Mascitti, V.R., "Calculation of Linearized Supersonic Flow Over Slender Cones of Arbitrary Cross Section", NASA TN D-6818, July, 1972.
10. Chan, Y.Y., "An Experimental Study of a Yawed Circular Cone in Hypersonic Flow", AIAA Journal, Vol. 7, No. 10, Oct. 1969, pp. 2035-2037.
11. Zakkay, V. and Visich, M., Jr., "Experimental Pressure Distribution on Conical Elliptic Bodies at $M_{\infty} = 3.09$ and 6.0", Polytechnic Institute of Brooklyn, PIBAL Report No. 467, March 1959.
12. Martellucci, A., "An Extension of the Linearized Characteristics Method for Calculating the Supersonic Flow Around Elliptic Cones", Journal of the Aeronautical Sciences, Vol. 27, No. 9, Sept. 1960, pp. 667-674.

REPORT DOCUMENTATION PAGE		READ INSTRUCTIONS BEFORE COMPLETING FORM	
1. REPORT NUMBER AFOSR-TR-79-0475	2. GOVT ACCESSION NO.	3. RECIPIENT'S CATALOG NUMBER	
4. TITLE (and Subtitle) SUPERSONIC FLOW PAST CONICAL BODIES WITH NEARLY CIRCULAR CROSS-SECTIONS	5. TYPE OF REPORT & PERIOD COVERED Final PART 111		
7. AUTHOR(s) Martin C. Jischke	8. CONTRACT OR GRANT NUMBER(s) AFOSR-77-3468		
9. PERFORMING ORGANIZATION NAME AND ADDRESS Aerospace, Mechanical & Nuclear Engineering University of Oklahoma Norma, Oklahoma 73019	10. PROGRAM ELEMENT, PROJECT, TASK AREA & WORK UNIT NUMBERS 2301/A6 61102F		
11. CONTROLLING OFFICE NAME AND ADDRESS AFOSR/NP Bolling AFB Wash DC 20332	12. REPORT DATE Oct 1978		
14. MONITORING AGENCY NAME & ADDRESS (if different from Controlling Office) OU-AMNE-78-10	13. NUMBER OF PAGES 62		
16. DISTRIBUTION STATEMENT (of this Report) Approved for public release; distribution unlimited.		15. SECURITY CLASS. (of this report) unclassified	
15a. DECLASSIFICATION/DOWNGRADING SCHEDULE			
17. DISTRIBUTION STATEMENT (of the abstract entered in Block 20, if different from Report)			
18. SUPPLEMENTARY NOTES			
19. KEY WORDS (Continue on reverse side if necessary and identify by block number)			
20. ABSTRACT (Continue on reverse side if necessary and identify by block number) See over			

Inviscid, supersonic conical flows past bodies whose cross-section deviates slightly from that of a right circular cone are studied by means of a perturbation technique. Writing the equation for the body as $\theta_b(\phi) = \theta_{0b} + \sum \theta_{nb} \cos n\phi + \sum \theta_{mb} \sin m\phi$, where $\theta_{nb}, \theta_{mb} \ll \theta_{0b}$, we have obtained analytical results with the assumption of a weak polar cross-flow (eg. $\vec{V} \cdot \hat{e}_\theta / a \ll 1$). The effects of small angles of attack and yaw are included. Using the hypersonic small disturbances theory approximations, we have developed explicit results for the flow field velocity components, pressure, entropy, and shock shape for cases $n, m = 1, 2, 3, 4$. Comparisons of theory with experiment for $n = 1, 2$ are favorable. The results obtained also agree with linearized theory when $M_1\theta \rightarrow 0$ and Newtonian theory when $M_1\theta \rightarrow \infty$. The streamsurfaces of the velocity field are calculated and possible waverider geometries that can be developed therefrom are discussed.

UNCLASSIFIED

SECURITY CLASSIFICATION OF THIS PAGE (When Data Entered)